ISSN 0280-5316
ISRN LUTFD2/TFRT--5787--SE

Towards an Understanding of the Dynamics and Energy Efficiency of the Human Heart by Mathematical Modelling

Patrik Hersenius

Department of Automatic Control
Lund University
February 2007

Department of Automatic Control
Lund Institute of Technology
Box 118
SE-221 00 Lund Sweden

Document name
MASTER THESIS

Date of issue
February 2007

Document Number
ISRNLUTFD2/TFRT--5787--SE

Author(s)
Patrik Hersenius

Supervisor
Håkan Arheden and Einar Heiberg at Clinical Physiology, Lund University Hospital
Rolf Johansson at Automatic Control in Lund

Sponsoring organization

Title and subtitle
Towards and Understanding of the Dynamics and Energy Efficiency of the Human Heart by Mathematical Modelling
(Ökad förståelse för hjärtats dynamik och energibevarande egenskaper genom matematiska modellering)

Abstract
This thesis is focused on modelling the pumping of the human heart. The modelling is limited to the left heart. Flows through the left heart were visualized by pathlines, streamlines and curl from 3D-velocity data acquired using 3D-velocity encoded magnetic resonance imaging (MRI). A mathematical model was developed based on control volume analysis, 3D-flow analysis and the latest developments in cardiovascular physiology. The mathematical model was implemented in Matlab/Simulink. This model allows the pulmonary vein, mitral and aortic flows and the corresponding kinetic energy to be calculated based on data extracted from cine and flow MRI using image analysis for the first time. The knowledge gaps in the research field of cardiovascular physiology made the theoretical identification of the system complex. A new way of interpreting the pumping mechanism by analysing concurrent events is introduced. A vortex in the left atrium is shown to store energy during systole. The return of the AV-plane during the fast filling phase is proposed to be influenced mostly by the kinetic energy of the retained flow and elastic strain energy of the heart and the large vessels. A high cardiac output experiment was also undertaken. This inspired to new theories concerning dynamic properties of the heart during exercise. In conclusion, the proposed approach enables quantification of the kinetic energy aspects of blood in human hearts.

Keywords

Classification system and/or index terms (if any)

Supplementary bibliographical information

ISSN and key title
0280-5316

ISBN

Language
English

Number of pages
70

Recipient's notes

Security classification

Contents

Chapter 1

Acknowledgements

The work behind this master thesis was carried out at the Department of Clinical Physiology at Lund University Hospital during the fall of 2006. First of all, I want thank Prof. Rolf Johansson at the Department of Automatic Control and Håkan Arheden at the Department of Clinical Physiology for coming up with this idea and giving me the opportunity of doing something this unique. Einar Heiberg, my supervisor, was truly fantastic in his commitment to this project. The outcome of the thesis relies on lots of useful inputs from everyone in the Cardiac MR Group involved in multidisciplinary discussions.

Chapter 2

Preliminaries

The theories behind the pumping mechanism of the heart have changed over the years as measurement and imaging technology have given physicians additional information. The new possibilities have not always been beneficial to the progressive development of cardiovascular physiology. The value of theories concerning local function need to be put in global context in order to be recognized.

This is a strange engineering problem since the heart is almost the optimal solution in a limited working range due to evolution. It would be hard to question the assumption that the energy loss has been minimized during millions of years. The complex structure of the heart makes it possible for every movement of every part to contribute to the total function in many more ways than the most obvious ones.

Visual examination of the heart based on observations of shape change will fall short when the function of the heart is to be explained. The heart is after all a pump and should be examined as a technical system. By calculating flows, kinetic energy and optimally pressures as well, secrets behind the pumping mechanism can be revealed.

The function of the heart is much more complex than an ordinary pump system. In order to focus on the most important properties, several assumptions were to be made before any measurements or modelling could begin. First of all, the heart must be studied and explained in its environment. This can be exemplified by the difference in function of the heart between horizontal and vertical body position. One important assumption in this thesis is that friction can be neglected. It is not that it is negligible as such, but it involves great uncertainties, and the interest of this work is to model a heart based on the maximum energy available in order to explain how energy can be stored and how the function of the heart can benefit from it. The magnitude of the work done by muscles is not of interest at this point since it is hard, if not impossible, to measure in its environment. At stationary heart rate, all of the available incoming kinetic energy of each cardiac cycle is assumed to be used or lost in the same cardiac cycle. This does not necessarily mean that it is the same energy as the incoming energy that is used, but an equal amount of energy. The effect of gravity on the blood inside of the heart is assumed to be cancelled out by buoyancy forces. The blood is considered to be incompressible and of constant density. The total blood volume is assumed to be constant over a short period of time.

The right and left heart are rather similar in function. By concentrating on the function of the left heart, the gain of this thesis will be greater than if the emphasis was put on the function of the heart as a whole. The function of the right heart can be

understood to a large extent by putting the findings of the left heart function into the context of the right heart.

Chapter 3

Problem description

The theories behind the pumping mechanism of the human heart have changed over the years as measurement and imaging technology have given physicians additional information. A realistic model of the human heart could open new possibilities in the understanding of the function of a healthy heart, put previous findings by others into context, and also contribute to the understanding of what ways that an unhealthy heart is limited in function.

3.1 Problem statement

How can the human heart be modelled with focus on dynamics and energy efficiency?

The specific goals of this thesis were:

- Create a foundation for future modelling of the pumping mechanism of the heart based on flows and energy.
- Generate hypotheses that can guide future research in order to fill gaps in cardiovascular physiology.

Chapter 4

Background

This chapter introduces the information that was the framework for this thesis. Section 4.1 describes the function of the heart as presented in the literature of cardiac basic physiology. This presentation differs compared to the physiological interpretation of the results in this thesis presented in Section 7.1. Section 4.2 presents the magnetic resonance imaging (MRI) based data acquisition techniques used.

4.1 Human heart

The human heart is divided into two halves, the left and the right heart, by the atrial and ventricular septum, see Figure 4.1. The halves are not symmetric. The left heart provides the systemic circulatory system with energy that makes the blood flow. The right heart has the corresponding function in the pulmonary circulatory system. The left heart consists of two cavities, the left atrium and the left ventricle, that are divided by the pressure controlled mitral valve. The left atrium has four inlets, the pulmonary veins. The left ventricle has one outlet, the pressure controlled aortic valve that is connected to the aorta. The right heart consists of two cavities, the right atrium and the right ventricle, that are divided by the pressure controlled tricuspid valve. The right atrium has two inlets, superior and inferior vena cavae. The right ventricle has one outlet, the pressure controlled pulmonary valve that is connected to the pulmonary artery. The atrio-ventricular-plane (AV-plane) is the plane that divides the heart in atria and ventricles [14]. The continuing description is focused on the left heart.

4.1.1 Physiology

The cardiac cycle is commonly divided into two main phases, systole and diastole. The mitral valve is closed during systole and open during diastole. Systole starts with the ventricular isovolumetric contraction that causes an increase in ventricular pressure. It is followed by a contraction of the ventricular muscular wall that pulls the AV-plane towards apex and ejects blood through the aortic valve to the aorta. Simultaneously, the incoming blood from the pulmonary veins is stored in the left atrium until the mitral valve opens in diastole. When the AV-plane has reached its bottom position, the isovolumetric relaxation takes place and the mitral valve opens. The myocardium is relaxed, which lets the AV-plane to move in basal direction and the left ventricle to expand as it is filled with the blood stored in the left atrium during systole and the

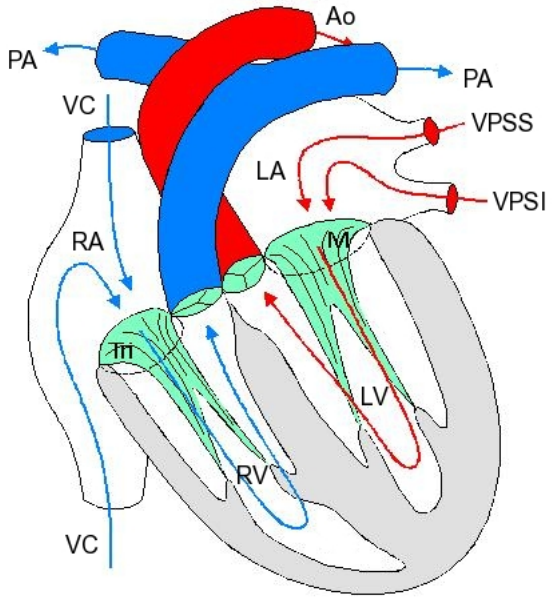

Figure 4.1: The anatomy of the human heart. LA - left atrium, LV - left ventricle, RA - right atrium, RV - right ventricle, PV - pulmonary vein (two of the pulmonary veins are hidden by the pulmonary artery), Ao - aorta, M - mitral valve, VC - vena cavae, PA - pulmonary artery and Tri - tricuspid valve. The image is used by permission [14].

pulmonary vein flow. The fast filling phase of diastole ends as the AV-plane movement stops. In late diastole, the atrium contracts and squeeze out a portion of the atrial blood volume and pulls the AV-plane even more in the atrial direction. The end of diastole is then followed by the next systole [14]. The phases of the cardiac cycle are illustrated in Figure 4.2 and 4.3.

The part of the ventricular muscular wall that is shared by the right and left ventricle is referred to as the ventricular septum. It balances the total stroke volume between the systemic circulatory system and the pulmonary circulatory system. When the ventricular muscular wall is relaxed during diastole, the position of the ventricular septum depends on the pressure difference between left and right ventricle [14, 20].

The volume of the muscular wall can be considered to be constant over the cardiac cycle. The total heart volume variation is limited to approximately 8% through the cardiac cycle [4]. The tip of the heart, apex, is almost fix through the cardiac cycle. The largest contribution to the stroke volume is caused by the movement of the AV-plane, which causes 60% of the stroke volume in the left heart and 80% in the right heart [5]. The volume change of the ventricles and the ventricular rotation are shown in Figure 4.4.

The impulse from the sinus node activates all muscle fibres in the heart. It reaches the atrium first and causes the atrial contraction. The ventricular contraction follows as the impulse reaches the ventricular wall. The size of the force generated depends, to

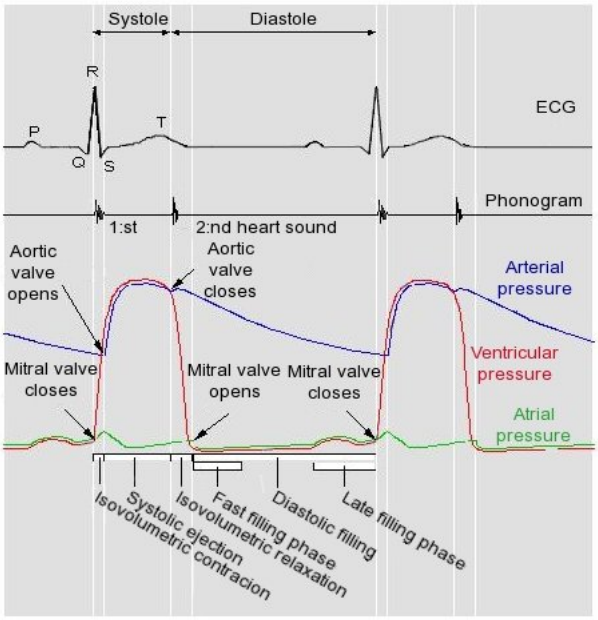

Figure 4.2: This illustration shows important concurrent events through the cardiac cycle. The QRS complex in the ECG-signal and the 1:st heart sound in the phonogram indicates start systole. The pressure of the left atrium (green), the left ventricle (red) and the arteries (blue) are shown through the cardiac cycle. This comparison is useful when analyzing factors that contribute to the flows. The image is used by permission [14].

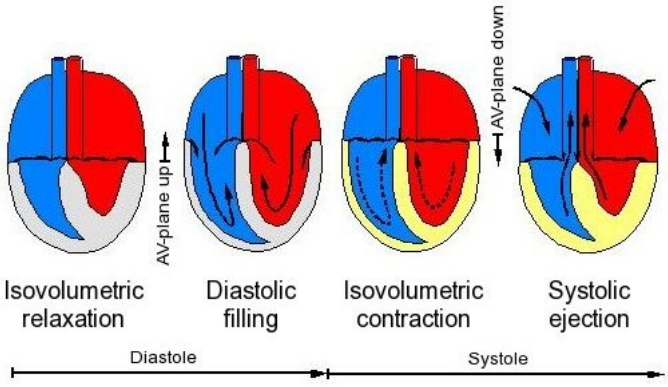

Figure 4.3: This image shows how the AV-plane is involved in the pumping mechanics of the heart. The ventricular muscular wall is active when it is yellow. The image is used by permission [14].

a large extent, on the intercellular concentration of calcium ions. The more a muscle fibre is extended, the more sensitive it gets to calcium ions. The force is built up of two

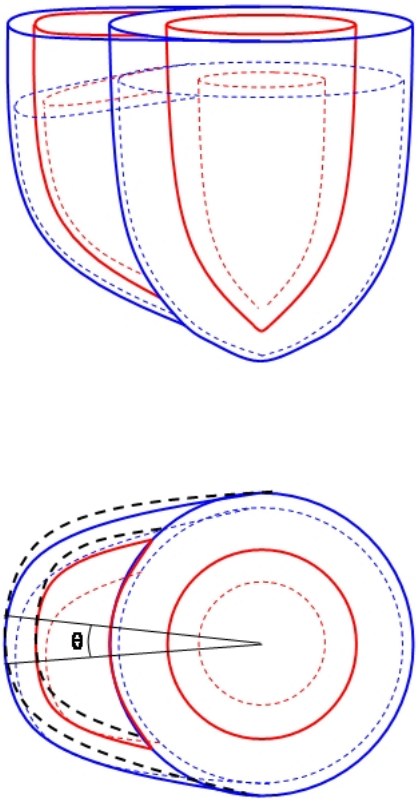

Figure 4.4: Volume change of the ventricles between end diastole (solid line) and end systole (dashed line). The endocardial volume is drawn in red and the epicardial volume is drawn in blue. The black dashed contour illustrates the apical rotation. The angle θ is the angle of the basal rotation relative apical rotation at end systole. The right ventricle is to the left and the left ventricle is to the right.

components, one active and one passive. The possible active contribution is related to the extension of the muscle, see Figure 4.5. The passive component is the elastic force of the muscle fibre and is similar to a spring force [14].

The internal viscosity of the myocardial fibres creates a large increase in friction for sudden changes in length. This resistance opposes abrupt inflow of blood but permits slower inflow [25].

The muscle fibre structure has been a topic of discussion for decades. The most complete model is the one of Ingels [13], which is illustrated in Figure 4.6. It is based on the fibre angles of different layers of the myocardium and the fact that a myocardial fibre has a limit in contraction/stretch of about 15% of its length. In order to explain the AV-plane stroke length, the myocardial layers can be summarized as an inner layer of fibres that spiral in a clockwise manner, a mid layer with circumferential fibres and an outer

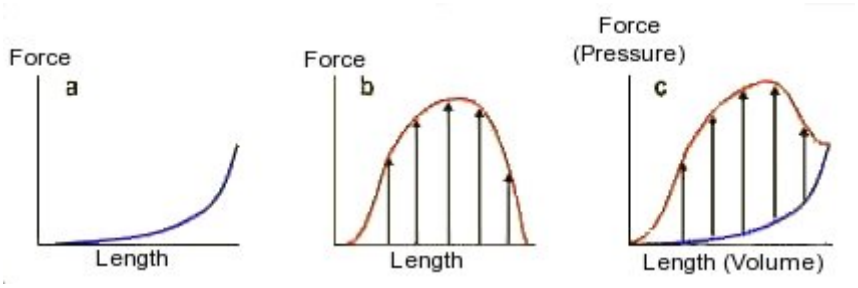

Figure 4.5: The left panel (a) shows the passive force component of a myocardial fibre, the panel in the middle (b) shows the corresponding active force component of a myocardial fibre and the right panel (c) shows the combined force. The image is used by permission [14].

layer with fibres that spiral counter clockwise. This setup allows an almost arbitrary stroke length due to shortening of the spiraling fibres. The mid layer is responsible of maintaining a high ventricular pressure. The myocardial contraction gives rise to torsion. The apex twists approximately 11 degrees relative the basal part of the ventricle, see Figure 4.4. Myocytes and groups of myocytes are covered with collagen weave and interconnected by collagen struts. Both of these collagen arrangements store elastic energy when deformed [13].

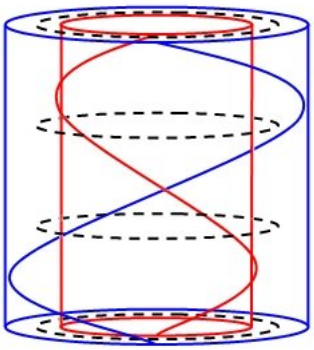

Figure 4.6: A simplified model of the muscle fibres in the left ventricle proposed by Ingels [13]. The blue muscle fibre is subepicardial, the dashed black fibres are circumferential and the red muscle fibre is subendocardial.

4.1.2 Heart from an energy perspective

The common opinion of the function of the left atrium is to be a reservoir during systole and a conduit during diastole [23, 29]. Vortex patterns in the atria has been proposed to store kinetic energy and to prevent stasis that could cause coagulation [8, 16, 17].

4.1.3 Cardiovascular system

In order to understand the function of the heart together with the complete systemic and pulmonary circulatory system, it is useful to follow the blood from the left heart all the way back to the left heart. During systole, blood of the left ventricle is ejected into the arteries that expand due to the change in volume and consequently, the pressure increases. The arteries are elastic and potential energy is stored during the expansion. The phenomenon is called the Wind-Kessel effect and acts as a lowpass filter for the flow and as an energy storage of the work done by the heart. The radii of the arteries are large enough to make the resistance low and the pressure uniformly distributed. The blood passes through the arterioles that are locally and sympathically controlled vents that distribute blood to organs and also try to maintain a constant pressure over the cardiac cycle. The arterioles have a major influence on the peripheral resistance, which is increased by arteriolar vasoconstriction and decreased by arteriolar vasodilation. After that the blood has been allocated by the arterioles, it enters the capillaries which are the passages where the exchange of nutrients and oxygen/carbon dioxide occurs. The combined cross section area of all capillaries is much greater than at any other point of the vascular system, which leads to a decrease in velocity. The radius of a capillary is about 20 times smaller than the radius of a hair. The red blood cells must be slightly deformed in order to pass through the capillaries. The next section of the systemic circulatory system is the ventrioles that can be considered as an extension of the capillaries. The last conduit before the blood enters the right atrium are the veins. They serve as the volume reserve of the vascular system and contain about 60% of the blood in the body. The pressure in the veins is almost constant over the cardiac cycle, but can change a little due to inspiration, skeletal muscle pumping work and sympathically controlled vasoconstriction. The resistance of the veins is low, so the pressure difference between the veins and the right atrium needed to make the blood flow is very small compared to pressure differences at other points in the vascular system. After that the blood has passed through the right heart, it reaches the lungs via the pulmonary artery and is oxygenated. The blood travels through the pulmonary veins and enters the left atrium. There is a small difference in pressure between the pulmonary veins and the atrium which can give rise to a flow due to the low resistance of the pulmonary veins. The circle is closed. The work of the heart together with the control mechanisms of the vascular system strive to keep a certain mean arterial pressure by controlling the heart rate and the peripheral resistance. The stretch sensitive baroreceptors in the arteries are the sensors that supply the medulary vascular centrum with information about the arterial pressure. The pressure is proportional to the firing frequency of the baroreceptors. There are also baroreceptors in the large systemic veins, the pulmonary vessels and in the walls of the heart which are used in feed forward control of the atrial pressure [28].

A premature beat can be the cause for a decrease in arterial pressure. This is compensated for by control of heart rate and peripheral resistance. When a certain mean arterial pressure is to be established, the control mechanisms in the vascular system vary the heart rate back and forth in order to box in the reference mean arterial pressure and to oppose transients [21]. The peripheral resistance is set simultaneously by nerve, hormoneous and locally controlled vasoconstriction/vasodilation. Peripheral resistance changes and heart rate must be synchronized with inspiration rate and the skelatal muscle pumping for optimal function. This is not done instantly and is especially evident in the beginning of a training session when exercising sports.

The flow of blood is laminar in most parts of the circulatory systems. The laminar

velocity profile of the blood differs slightly from the one of a homogenous incompressible fluid. The layers closest to the wall of the vessel consists of plasma. The blood cells are concentrated to the center of the vessel which makes the velocity profile smoother [25].

4.1.4 Heart and its surroundings

The importance of studying the heart in its environment was proposed by Lundbäck [20]. The surroundings contribute passively to the function of the heart which makes organ bath studies of limited interest. An example is that the change in total heart volume must be compensated for by displacement of adjacent tissue since tissue has incompressible fluid-like properties. The inertia of the adjacent tissue will oppose such displacement partly, which makes volume variations expensive from an energy perspective. This was the base for the research that introduced the AV-plane movement as the main contributor to the ventricular ejection.

4.1.5 Cardiovascular system during exercise

The cardiac output of healthy adults spans from a couple of litres per minute at rest to 15-20 L/min during exercise. The cardiac output of some athletes can reach 35 L/min during exercise [20]. Consequently, there has to be different working modes of the heart in order to deliver the volumes mentioned above. The studies of Kilner *et al* [15] show that the aortic valve is partly open in diastole and that the mitral valve is partly open during systole at heart rates of 120 bpm and more. The AV-plane displacement has a sinusoidal pattern at these heart rates. During exercise, the major contributors to changes in venous pressure are the skeletal-muscle pump and inspiration [10, 28].

4.1.6 Gaps in the physiology of the heart

When reviewing the knowledge of the physiology of the heart, there are appreciable gaps in the understanding of the basic physiology. What functions contribute to the flow? Is the stroke volume really inflow controlled when the heart is enclosed in thorax as the organ bath based Frank-Starling law states? Does the valves function as discrete vents or are they dynamic? How does the function of the heart change between rest and exercise? Are there any benefits from the total heart volume variation? What is the function of the atrium? What flow structures exist in the heart and why? What mechanisms are involved in the fast return of the atrio-ventricular plane?

4.2 Magnetic resonance imaging

In this section, the basics of magnetic resonance imaging are explained. The development of Magnetic Resonance Imaging, or short MRI, is based on Nuclear Magnetic Resonance (NMR). In order to separate this imaging technique from other imaging techniques that involve ionizing radiation, the word nuclear is commonly left out.

In order to have a frame of reference, a orthogonal cartesian coordinate system, xyz, is used. Imagine a person in supine position on a bunk, then z is in the direction from feet to head, x is in the direction from left hand to right hand and y is parallel to the sagittal plane.

4.2.1 Nuclear magnetic resonance

Nuclear magnetic resonance is based on the angular momentum of nucleus that exists in atoms with odd nucleon numbers. In medicine, the focus has been mainly on the spin properties of the hydrogen atom due to its abundance in the human body. The spin of a proton or a neutron can be either in the high energy state (spin-up) or the low energy state (spin-down). The nucleons try to pair with nucleons of the same kind, but with opposite spin, in order to minimize the energy. In nuclei with an odd number of nucleons, this cancellation of spins is not possible and it gives rise to a net angular momentum and a magnetic dipole moment.

When nucleus with magnetic dipole moments are placed in a static magnetic field, they align to the magnetic field in a certain way. The nuclei of hydrogen, a proton, is a 1/2-spin particle and aligns to either precess about an axis parallel (low energy state) or to precess about an axis anti parallel (high energy state) to the magnetic field. The frequency that the nuclei is precessing with is the Larmor frequency which is given by

$$\omega_0 = \gamma B_0 \tag{4.1}$$

where γ is the gyromagnetic ratio and B_0 is the applied magnetic field. For hydrogen, the gyromagnetic ratio is

$$\gamma_{\text{hydrogen}} = 42.58 \, \frac{[\text{MHz}]}{[\text{T}]} \tag{4.2}$$

The population difference between protons that precess parallel and anti-parallel is governed by Boltzmann statistics. The greater abundance of low energy state protons causes a net magnetisation vector $\mathbf{M}$ that is parallel to the magnetic field.

If a radio pulse, a so called RF-pulse, is send out with a bandwidth that covers the Larmor frequency of the nucleus in question, the steady state equilibrium between high and low energy state nucleus will be perturbated. The nucleus will now precess in phase. Some low energy nuclei are excited to a temporary non-aligned high energy state. This causes an altered population difference and thus a change of the net magnetisation vector. By adjusting the magnitude of the RF-pulse, the angle of the net magnetisation vector can be changed to an arbitrary flip angle.

The excited nucleus dephase and deexcite and consequently, the equilibrium population difference is restored. During the relaxation, a signal is generated in the detection coils of the MR-scanner, the free induction decay signal. The signal decreases as the net magnetization vector is restored to its equilibrium direction. The relaxation is given by the Bloch equation

$$\frac{d\mathbf{M}}{dt} = \mathbf{M} \times \mathbf{B} - \frac{M_x}{T_2}\hat{\mathbf{x}} - \frac{M_y}{T_2}\hat{\mathbf{y}} - \frac{M_z - |\mathbf{M}|}{T_1}\hat{\mathbf{z}} \tag{4.3}$$

where T_1 is the relaxation time that descripes how fast the equilibrium population difference is restored. T_2 is the relaxation time that describes the time required for the spins to get out of phase. $T_1 > T_2$. The relaxation times differ between different kinds of tissue, which is a necessity in order to obtain useful information.

The MR-scanner creates a strong homogenous magnetic field, B_0, in z-direction which causes the alignment of the axis of the precessing nucleus. In order to spatially distinguish voxels at different positions in the body, three magnetic gradients are used. They are aligned to the xyz-coordinate system.

$$G_x = \frac{\delta B}{\delta x}, G_y = \frac{\delta B}{\delta y}, G_z = \frac{\delta B}{\delta z} \tag{4.4}$$

This leads to local differences in Larmor frequency

$$\omega = \gamma(B_0 + \mathbf{G} \cdot \mathbf{r}) \tag{4.5}$$

where ω is the Lamour frequency, $\mathbf{G}$ is the gradient and $\mathbf{r}$ is the position of the proton.

4.2.2 Signal encoding

The positive G_z gradient is applied as the RF-pulse is send out. This gradient makes the RF-pulse to only excite protons in a certain slice in the xy-plane. The thickness of the slice is determined by the bandwidth of the RF-pulse. After the RF-pulse, the G_z gradient is mirrored in the xy-plane and scaled in order to provide a uniform signal strength within the slice. This is followed by applying a negative G_x gradient that changes the frequency of the spins for different positions on the x-axis. Simultaneously, a positive G_y gradient is applied shortly which causes a difference in phase of the spins at different locations in y-direction.

In balanced steady state free precession (SSFP), which is the sequence used in cine imaging and real time imaging, the phase of the spins are changed 180^o by the RF-pulse every sample which is equal to alternate the flip angle between α and $-\alpha$. A choice of T_1 and T_2 that makes the ratio $\frac{T_2}{T_1}$ large gives good image contrast.

The sequence of 3D-MRI is similar to the 2D-technique described above. The greatest difference is a G_z gradient that is applied at the same time as the G_y in order encode the phase of the spins in z-direction as well.

The fast field echo sequence used in flow MRI uses a gradient in the direction of the flow, which encodes the matter by phase, which is proportional to the velocity in the direction perpendicular to the measurement plane [22]. By letting a positive gradient to be followed by a negative gradient, it is possible to remove the contributions from still standing protons by subtracting the phase encoded images. The velocity encoding (VENC) determines the highest velocity possible to be detected without aliasing effects.

4.2.3 Signal detection

In the gradient echo sequence, the RF-pulse generates a flip angle α of the net magnetisation vector. In the decoding phase, a positive G_x gradient is applied that dephases the spins and a signal can be detected in the detecting coils. The echo time of the gradient method is rather short compared to sequences like spin echo. This gives a high temporal resolution at the cost of signal strength.

Retrospective triggering is used in cine, flow and 3D-flow MRI, which means that the data gets a time stamp that indicates when the data was encoded relative to the R-tag in the ECG signal. This is used in order to fit the image data from several cardiac cycles into a sequence of images covering one cardiac cycle. Triggering is not used in real time imaging.

4.2.4 Image reconstruction

The detected signal S(t) equals the Fourier transform of the effective spin density ρ_{eff}.

$$S(t) = \tilde{\rho}_{\text{eff}}(\mathbf{k}(t)) \equiv \iiint \rho_{\text{eff}}(\mathbf{x}) \cdot e^{2\pi\imath\ \mathbf{k}(t)\cdot\mathbf{x}} d\mathbf{x} \tag{4.6}$$

where

$$\mathbf{k}(t) \equiv \int_0^t \mathbf{G}(t')\ dt' \tag{4.7}$$

The k-space, $S(\mathbf{k})$, is a two-dimensional matrix in 2D-MRI and a three-dimensional matrix in 3D-MRI. The inverse Fourier transform of the acquired data gives the image

$$I(\mathbf{x}) = \iiint S(\mathbf{k}(t)) \cdot e^{-2\pi\imath\ \mathbf{k}(t)\cdot\mathbf{x}} d\mathbf{k} \tag{4.8}$$

The field of view of the image is given by

$$FOV \propto \frac{1}{\Delta k} \tag{4.9}$$

and the resolution is given by

$$\text{Resolution} \propto |k_{\max}| \tag{4.10}$$

Chapter 5

Methods

This chapter describes the experimental setup, the approach for analyzing 3D-flow data and how the dynamics of the heart were modelled.

5.1 MRI - Data acquisition

Magnetic resonance imaging (MRI) was used in order to measure flow and motion in the human body. Two MRI-scanners (Philips Intera, Best, the Netherlands), with field strength 1.5T and 3T respectively, were used for data acquisition. Both scanners were equipped with cardiac synergy coils. The experiments performed were 3D-flow, flow and cine imaging of two healthy volunteers, subject A and B.

The setup for subject A was 1.5T MRI-scanner for cine imaging, 1.5T MRI-scanner for flow imaging and 3T MRI-scanner for 3D-flow imaging.

The setup for subject B was 3T MRI-scanner for cine imaging, 3T MRI-scanner for flow imaging, 3T MRI-scanner for realtime flow imaging and 3T MRI-scanner for 3D-flow imaging. Setup for physical work in the MR-scanner: A harness was put on the subject and elastic rubber bands were attached to the harness and the feet. The harness was fastened to the bunk. The work was done by extending the elastic bands horisontally by stretching both legs simultaneously with a table as vertical support for the feet. Real time MRI was used in this experiment.

The sequence details were:

- 1.5T 2D-cine imaging: Steady state free precession sequence with retrospective ECG triggering, temporal resolution: $\approx$ 30 ms (longaxis 20 ms), spatial resolution: 1.4x1.4x8 mm, repetition time: 2.8 ms, echo time: 1.4 ms, flip angle: 60 °. All cine images were aquired during end-expiratory apnea.

- 1.5T 2D-flow imaging: Free breathing fast field echo velocity encoded with retrospective ECG triggering, temporal resolution: 20-35 ms, slice thickness: 6 mm, in plane spatial resolution: 1.2x1.2 mm, repetition time: 10 ms, echo time: 5 ms, flip angle: 15 °, number of phases: 35, number of acquisitions: 1, velocity encoding: 200 cm/s (aorta and mitral valve) and 80 cm/s (veins). All of the flow image planes were placed perpendicular to the vessel of interest.

- 3T 2D-cine imaging: Steady state free precession sequence with retrospective ECG triggering, , temporal resolution: 33 ms, spatial resolution: 1.4x1.4x8mm, repetition time: shortest, echo time: shortest, flip angle: 40 °, number of phases: 30, number of acquisitions: 1. All cine images were aquired during end-expiratory apnea.

- 3T 2D-flow imaging: Free breathing fast field echo velocity encoded with retrospective ECG triggering, temporal resolution: 29 ms, slice thickness: 6 mm, in plane spatial resolution: 1.2x1.2 mm, repetition time: shortest, echo time: shortest, flip angle: 40 °, number of phases: 35, number of acquisitions: 1, velocity encoding: 200 cm/s (aorta and mitral valve) and 80 cm/s (veins). All of the flow image planes were placed perpendicular to the vessel of interest.

- 3T 2D-real time flow imaging: Free breathing fast field echo velocity encoded, fast imaging mode: EPI , temporal resolution: shortest, slice thickness: 10 mm, in plane spatial resolution: 1.2x1.2 mm, repetition time: shortest, echo time: shortest, flip angle: 20 °, number of scans: 100, velocity encoding: 180 cm/s. The flow image plane was placed perpendicular to the aorta.

- 3T 3D-flow imaging [32]: Free breathing turbo field echo velocity encoded with retrospective ECG triggering, temporal resolution: 63 ms, slice thickness: 3 mm, repetition time: shortest, echo time: 3.70 ms, flip angle: 8 °, number of phases: 16, number of acquisitions: 1, phase contrast velocity encoding: 100 cm/s , contrast enhancement: T1 .

5.2 Image analysis

In order to extract useful information from the images acquired with the MR-scanners, segmentation and object tracing were done using the freely available cardiac imaging analysis software Segment (http://segment.heiberg.se).

5.2.1 Segmentation of flow data

The first step was to identify the vessel and to outline a stationary region of interest. It was done by using an anatomical image and a velocity magnitude image of a plane perpendicular to the vessel, see Figure 5.1. The region of interest was made time resolved by using the automatic flow based refinement method in Segment [12]. The segmentation was refined manually to ensure that the region of interest was the contour of the cross section of the vessel in every timeframe.

5.2.2 AV-plane position

Three different long axis images, LVOT, two-chamber and four-chamber, were used in order to provide data for an estimate of the position of the atrio-ventricular plane (AV) relative to the apex. In each of the images, a centered straight line was drawn in the left ventricle that was parallel to the movement of the AV-plane. Two fix annotation points were placed in apex, one at each side of the line. One time resolved annotation point was placed on each side of the central line, in the region where the AV-plane is attached to the myocardium. The position of the apical points was chosen so that the distance

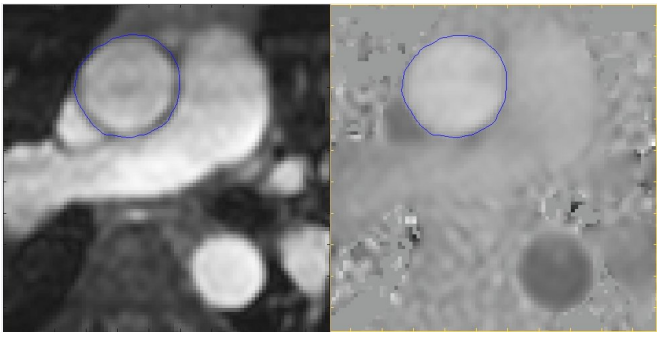

Figure 5.1: Aorta at flow peak in systole. An anatomical image to the left and a phase image containing velocity information to the right. The blue contour is the region of interest for the ascending aorta.

to the central line was approximately the same as the distance from the corresponding time resolved point on each side to the central line, see Figure 5.2.

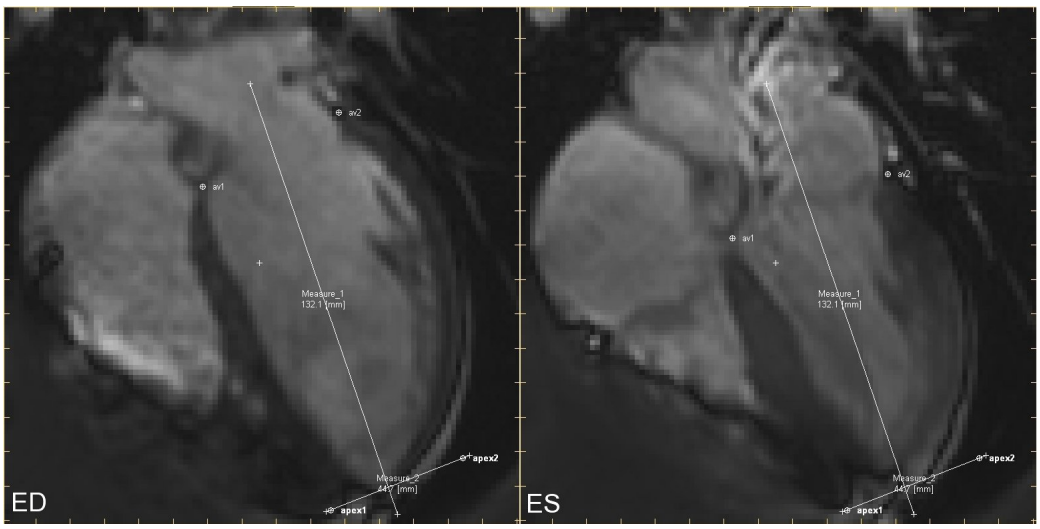

Figure 5.2: A four-chamber image at end diastole to the left and the corresponding image in end systole to the right. The movement of the AV-plane is tracked by the time resolved annotation points, av1 and av2.

5.3 3D flow analysis

The commercially available 3D-visualization software Ensight 8.2 was used to visualize the properties of the flow of blood in the heart based on 3D-flow images. To visualize three dimensional flow fields of the heart the use of particle trace technique has been proposed [31].

5.3.1 Flow visualization

Pathlines were used to visualize the flow of blood from the pulmonary veins through the left heart. A pathline is defined as

$$\frac{d\mathbf{x}}{dt} \equiv \mathbf{u}(\mathbf{x}, \mathrm{t}) \tag{5.1}$$

where $\mathbf{u}(\mathbf{t})$ is the velocity and $\mathbf{x}(\mathrm{t}_0) = \mathbf{x}_0$ is the initial position. It is a trace of a virtual massless particle in a time varying velocity field. The pathline was colored by either time or velocity. The blood of the mitral flow and aortic flow were traced by creating pathlines backwards in time. Depending on color code, the pathline gives information about where the blood comes from, when it passes certain points or at what velocity it passes certain points. Unfortunately, Ensight has no support for backward integration in time so a trick had to be done. The index of the starting file was chosen to be the last timeframe and the time increment was changed from 1 to -1 in the case file. A new variable was created in Ensight, the negative velocity. The combined effect of the changes and the new variable was

$$\mathbf{v}_{\mathrm{new}}(\mathbf{x}(\mathrm{i}), \mathrm{i}) = -1 \cdot \mathbf{v}(\mathbf{x}(\mathrm{k}_{\max} - \mathrm{k}), \mathrm{k}_{\max} - \mathrm{k}) \tag{5.2}$$

where k is the timeframe in forward time, i is the time frame backwards in time and x is the position. $i = k_{\max} - k,\ 0 < i < i_{\max},\ 0 < k < k_{\max}$

5.3.2 Orientation in the 3D-volume

Before any post processing could be done, it was necessary to get a picture of what to trace, where it occurs and when it occurs. By using several clip planes with velocity colormaps it was possible to place one short axis plane, one two-chamber long axis plane and one four-chamber long axis plane in a way that made it easy to identify the left ventricle. Three perpendicular clip planes were created in the left atrium. By translating the planes, each of the pulmonary vein inflow tracts could be located in the systolic peak time frame. In order to locate the mitral valve, backward pathlines were used. The initial position of the path was chosen to be in the upper part of the left ventricle and the initial time was the mitral flow peak in diastole. The size of the emitter plane was chosen to be small enough not to trace any particles outside of the mitral flow. If some traces pointed in the apical direction, the emitter plane was translated in basal direction and the procedure was repeated. Aorta was located by searching for the largest velocities in the left ventricle outflow tract in mid systole.

5.3.3 Vortex identification

In order to identify a vortex, vector planes and the curl were used. A vector plane was placed perpendicular to the axis of the supposed vortex caused by the incoming pulmonary vein flow. The pathlines of the pulmonary vein flow were used to make the orientation easier. The vector plane was chosen to show curvilinear streamlines. A streamline is defined as

$$\frac{d\mathbf{x}}{ds} \equiv \mathbf{u}(\mathbf{x}) \tag{5.3}$$

where s is a variable that parametrizes the curve s on $\mathbf{x}(\mathbf{s})$ and $\mathbf{u}(\mathbf{x})$ is the velocity vector in position $\mathbf{x}(\mathbf{t})$ at a constant time t. Streamlines are not time dependent, so the

result should be interpreted as steady state particle traces. The curl of the velocity in a certain plane was studied in order to get more information about vortex properties. The curl is a vector that points in the direction of the axis of a rotating volume. The length of the vector is related to the strength of the vortex. The right hand rule can be used to illustrate the curl. The direction of the thumb is the positive direction of the curl if the hand is shaped so that the fingers point in the direction of the flow. The curl is defined as

$$\nabla \times \mathbf{v} \equiv \text{curl}(\mathbf{v}) \tag{5.4}$$

where $\mathbf{v}$ is the velocity [24].

5.4 Conceptual model of the pumping mechanics

The cardiac contraction performs work that is not released instantly. In order to model this, the concept of elastic strain energy was introduced. The work done by the heart does not only cause the blood to flow instantaneously, but also to make it continue flowing, at least until the next ventricular contraction. All together, the released potential energy is called elastic strain energy [1]. It is most important during the fast filling phase in diastole due to the absence of muscular work. This section describes all of the different mechanisms that we have identified as potential contributions to elastic strain energy. The mechanisms will be discussed and explained upon in the interpretation of the results of the experiments.

Spring forces
Spring forces of unknown size are built up in the aorta and the pulmonary artery during ventricular contraction as the AV-plane moves towards apex. The spring forces that are built up in the left atrium simultaneously are of limited size since the auricles are unfolded with minimal stretching [20]. Collagen in the ventricular wall stores elastic energy when deformed [13]. Another spring force is the passive force component of the left ventricular muscular wall that will increase in size as the muscular wall is extended when the atrial contraction moves the AV-plane in basal direction [14].

Torsion
The deformation of the left ventricle during ventricular contraction can be subdivided into three contributions, radial compression, long axial compression and torsion [13]. The ventricular contraction makes apex to rotate relative the basal part of the left ventricle. As work is done during the contractions, the heart and the circulatory systems are deformed. When the muscles relax, the heart returns to its undeformed state and stored potential energy that is equal in magnitude to the applied work that caused the deformation is released. In order to model the effect of torsion to the function of the heart, the apical/basal twist will be modelled as torsion of a hollow shaft.

The polar 2nd moment of area for the circular hollow shaft is given by

$$J = \int_{r_2}^{r_1} 2\pi r^3 dr = \frac{\pi}{2}\left(r_1^4 - r_2^4\right) \tag{5.5}$$

where r_1 is the outer radius and r_2 is the inner radius [1]. The torsion T is given by

$$T = \frac{\tau}{r_1}\frac{\pi}{2}\left(r_1^4 - r_2^4\right) \tag{5.6}$$

where τ is the shear stress [1]. For torsion, the following relations hold

$$\frac{T}{J} = \frac{\tau}{r} = \frac{G\theta}{L} \tag{5.7}$$

where L is the length of the shaft, G is the shear modulus and θ is the angle that describes the rotation of apex relative the basal part of the left ventricle in cylindrical coordinates, see Figure 4.4. The relation between the angle θ and the torsion T is

$$K = \frac{T}{\theta} \tag{5.8}$$

where K is a constant. It can be rewritten as Hookes law

$$T = K\,\theta \tag{5.9}$$

Pressure differences

If there are pressure differences between different regions of a volume, the potential energy of particles will depend on location. In this way, thermodynamics can be used in order to explain the properties of the volume that encloses the blood, the circulatory systems. This choice of approach makes it possible to describe the circulatory systems in a strict way by looking at a suitably detailed level. The total inner volume of the mechanical system is fix on a small time scale, in other words, there is no dramatic change of the total blood volume during a short period of time unless bleeding occurs [20]. The total volume can be divided into four subsystems, the left heart, the right heart, the pulmonary circulatory system and the systemic circulatory system. The change of volumes between the systems depend on the pressure difference or the work applied, and can occur both as flow and as shape change of a membrane. For the volume of the subsystems it holds that

$$dV_{\text{left heart}} = -\left(dV_{\text{pcs}} + dV_{\text{scs}} + dV_{\text{right heart}}\right) \tag{5.10}$$

where $V_{\text{left heart}}$ is the volume of the left heart, V_{pcs} is the volume of the pulmonary circulatory system, V_{scs} is the volume of the systemic circulatory system and $V_{\text{right heart}}$ is the volume of the right heart. The total entropy S_{tot} is a function of energy and volume of all of the subsystems since they are related. Equilibrium is obtained when S_{tot} is maximized and that occurs when

$$\frac{\delta S_{\text{left heart}}}{\delta V_{\text{left heart}}} = \frac{\delta S_{\text{right heart}}}{\delta V_{\text{right heart}}} = \frac{\delta S_{\text{pcs}}}{\delta V_{\text{pcs}}} = \frac{\delta S_{\text{scs}}}{\delta V_{\text{scs}}} \tag{5.11}$$

where $S_{\text{left heart}}$ is the entropy of the left heart, S_{pcs} is the entropy of the pulmonary circulatory system, S_{scs} is the entropy of the systemic circulatory system and $S_{\text{right heart}}$ is the entropy of the right heart [26]. During systole and the slow filling phase of diastole, work is done that changes the distribution of blood between the systems and consequently, the entropy is reduced. The left heart volume variation is given by

$$V_{\text{LHVV}} = -\int_0^T q_{\text{aorta}}dt + \sum_{i=1}^{4}\int_0^T q_i dt \tag{5.12}$$

where q_{aorta} is the aortic outflow and q_i is the inflow of each of the four pulmonary veins. The right heart volume variation is given by

$$V_{\text{RHVV}} = -\int_0^T q_{\text{pa}} dt + \sum_{j=1}^{2} \int_0^T q_j dt \tag{5.13}$$

where q_{pa} is the pulmonary artery outflow and q_j is the inflow of each of the two vena cavas. Combined, the left heart volume variation and the right heart volume variation are the total heart volume variation, V_{THVV} [4].

$$V_{\text{THVV}} = V_{\text{LHVV}} + V_{\text{RHVV}} \tag{5.14}$$

The pulmonary circulatory system volume variation is given by

$$V_{\text{PCSVV}} = \int_0^T q_{\text{pa}} dt - \sum_{i=1}^{4} \int_0^T q_i dt \tag{5.15}$$

where q_{pa} is the pulmonary artery inflow and q_i is the outflow of each of the four pulmonary veins. The systemic circulatory system volume variation is given by

$$V_{\text{SCSVV}} = \int_0^T q_{\text{aorta}} dt - \sum_{j=1}^{2} \int_0^T q_j dt \tag{5.16}$$

where q_{aorta} is the aortic inflow and q_j is the outflow of each of the two vena cavas.

5.5 Flow model of the left heart

Control volume analysis was used in order model the physical behaviour of the left heart by using Reynolds Transport Theorem as a base for balance equations of mass, linear momentum, angular momentum and energy. The equations balance the changes inside of a control volume with the fluxes through the control surface [30]. The balance equations of angular momentum and linear momentum were used in order to give a picture of the system, not for calculations. The left heart was divided into two control volumes, the left atrium and the left ventricle. The heart changes shape and moves over time, so the control volumes were chosen to be deformable and relative velocities were taken into account. The blood was considered to be incompressible. Before the analysis could start, some definitions had to be made. $\mathbf{v}_r$ is the relative velocity, $\mathbf{v}_s$ is the velocity of a control surface and $\mathbf{v}$ is the velocity in eulerian coordinates. They are related by

$$\mathbf{v}_{\text{r}}(\mathbf{x}, \text{t}) = \mathbf{v}(\mathbf{x}, \text{t}) - \mathbf{v}_{\mathbf{s}}(\mathbf{x}, \text{t}) \tag{5.17}$$

where $\mathbf{x}$ is the position. For the pulmonary veins, it holds that

$$\mathbf{v}_{\text{r}}(\mathbf{x}, \text{t}) \approx \mathbf{v}(\mathbf{x}, \text{t}) \tag{5.18}$$

but for the mitral valve, the situation is different since the valve moves a lot itself

$$\mathbf{v}_{\text{r}}(\mathbf{x}, \text{t}) \neq \mathbf{v}(\mathbf{x}, \text{t}) \tag{5.19}$$

The impact of the behaviour of the mitral valve on the change of volume between the left atrium and the left ventricle has to do with flow in eulerian coordinates and the change of borders caused by the mitral movement, which has been denoted the mitral annular excursion volume, [3]. The relative velocity was only used in order to balance mass. The state of the mitral valve is described as a logic switch $\varphi_{\text{mitral}}(t)$ that is either open or closed during normal conditions at rest. 1 corresponds to fully open.

$$\varphi_{\text{mitral}}(t) = \begin{cases} 0 & t \in \text{systole} \\ 1 & t \in \text{diastole} \end{cases}$$

Aorta does also move with the AV-plane. The relative velocity will be used for mass balance and absolute velocity in all other cases. For the aorta it holds that

$$\mathbf{v}_{\text{r}}(\mathbf{x}, \text{t}) \neq \mathbf{v}(\mathbf{x}, \text{t}) \tag{5.20}$$

5.5.1 Left atrium

The left atrium is modelled as a moving deformable control volume with four inlets/outlets, the pulmonary veins and one outlet, the mitral valve.

Mass conservation

The time derivative of the system mass is equal to the difference between the change of control volume mass over time and the mass flow through the four pulmonary veins and the mass flow out of the control volume through the mitral valve. The mass balance equation is given as

$$\begin{aligned} \frac{d}{dt}\left(m\right)_{\text{system}} =& \frac{d}{dt}\left(\int_{LA} \rho dV\right) + \sum_{i=1}^{4}\left(\int \rho\left(\mathbf{v}_r \cdot \hat{\mathbf{n}}\right) dA_i\right) \\ &+ \varphi_{\text{mitral}}(t) \int \rho\left(\mathbf{v}_r \cdot \hat{\mathbf{n}}\right) dA_{\text{mitral}} = 0 \end{aligned} \tag{5.21}$$

where m is the mass of the inner volume of left atrium, ρ the density of the blood, $\mathbf{v}_{\text{r}}$ is the relative velocity, $\hat{\mathbf{n}}$ is the surface normal and φ_{mitral} is the mitral valve function.

Linear momentum relation

The linear momentum relation answers to how energy will be distributed in the system. The change of linear momentum of the system over time is given by

$$\frac{d}{dt}\left(m\mathbf{v}\right)_{\text{system}} = \sum \mathbf{F} - \int_{\text{LA}} \mathbf{a}_{\text{r}} dm = 0 \tag{5.22}$$

where the first term on the right hand side is the sum of forces acting on the system and the second term is Newton's second law applied to a moving system with a relative acceleration, $\mathbf{a}_{\text{r}}$, which is given by

$$\mathbf{a}_{\text{r}} = \frac{d^2\mathbf{R}}{dt^2} + \frac{d\boldsymbol{\Omega}}{dt} \times \mathbf{r} \tag{5.23}$$

where the first term on the right hand side is the acceleration of the origin **R** of a relative coordinate system and the second term is the angular acceleration effect in eulerian coordinates and **Ω** is absolute angular velocity.

The mass of the walls can be seen as infinite since they are supported by the surrounding tissue [20]. By combining this and the assumption that the inner walls of the heart are streamlined, the losses of kinetic energy of the blood to the walls will be limited. By applying Reynolds Transport Theorem to linear momentum, the equation takes the form.

$$\begin{aligned}\frac{d}{dt}\left(m\mathbf{v}\right)_{\text{system}} =& \frac{d}{dt}\left(\int_{\text{LA}} \mathbf{v}\rho dV\right) + \sum_{i=1}^{4}\left(\int \mathbf{v}\rho\left(\mathbf{v}_{\text{r}}\cdot\hat{\mathbf{n}}\right)dA_i\right) \\ &+ \varphi_{\text{mitral}}(t)\int \mathbf{v}\rho\left(\mathbf{v}_{\text{r}}\cdot\hat{\mathbf{n}}\right)dA_{\text{mitral}}\end{aligned} \tag{5.24}$$

where m is the mass of the inner volume of the left atrium, ρ the density of the blood, $\mathbf{v}$ is the absolute velocity, $\mathbf{v}_{\text{r}}$ is the relative velocity, $\hat{\mathbf{n}}$ is the surface normal and φ_{mitral} is the mitral valve function.

Angular momentum relation

The angular momentum relation shows whether the control volume opposes a possible torque caused by the inflows/outflows or not. If the left atrium would not oppose the torque, the whole volume would rotate. The angular momentum of the system is the mass integral of the angular moments of every elemental mass dm within the system about an arbitrary point **P** . The angular moment is defined as

$$\mathbf{H}_P = \int_{\text{system}} \left(\mathbf{r}\times\mathbf{v}\right)dm \tag{5.25}$$

where **r** is the distance between point **P** and the elemental mass dm. The change of angular momentum of the left atrium over time is the torque and is given by

$$\frac{d\mathbf{H}_P}{dt} = \sum\left(\mathbf{r}\times\mathbf{F}\right)_P - \int_{\text{LA}}\left(\mathbf{r}\times\mathbf{a}_{\text{r}}\right)dm \tag{5.26}$$

where the first term on the right hand side is the sum of moments acting on the system and the second term is the relative torque based on Newton's second law applied to a moving system with a relative acceleration $\mathbf{a}_{\text{r}}$.

By applying Reynolds Transport Theorem to angular momentum, the torque equation takes the form

$$\begin{aligned}\frac{d\mathbf{H}_P}{dt} =& \frac{d}{dt}\left(\int_{\text{LA}}\left(\mathbf{r}\times\mathbf{v}\right)\rho dV\right) + \sum_{i=1}^{4}\left(\int\left(\mathbf{r}\times\mathbf{v}\right)\rho\left(\mathbf{v}_{\text{r}}\cdot\hat{\mathbf{n}}\right)dA_i\right) \\ &+ \varphi_{\text{mitral}}(t)\int\left(\mathbf{r}\times\mathbf{v}\right)\rho\left(\mathbf{v}_r\cdot\hat{\mathbf{n}}\right)dA_{\text{mitral}}\end{aligned} \tag{5.27}$$

where the first term on the right hand side is the torque that the control volume has to balance out the applied torques with, if the control volume should stay in its original position, the second term on the right hand side is the sum of the contributions of the

pulmonary vein flows to the total torque about point **P** and the third one is the mitral contribution. The left atrium will change shape and position, but unbalanced torque is not one of the big causes.

Energy equation

The time derivative of the applied work must balance the change of energy of the left atrium in the following way

$$\frac{dQ}{dt} - \frac{dW}{dt} = \frac{dE}{dt} \tag{5.28}$$

where Q is heat, W is the applied work and E is the energy. In order to analyse energy relations with Reynolds Transport Theorem, the following equation is used

$$\begin{aligned} \frac{dE}{dt} =& \frac{d}{dt}\left(\int_{LA} e\rho dV\right) + \sum_{i=1}^{4}\left(\int e\rho\left(\mathbf{v}\cdot\mathbf{n}\right)dA_i\right) \\ &+ \varphi_{\text{mitral}}(t)\int e\rho\left(\mathbf{v}\cdot\hat{\mathbf{n}}\right)dA_{\text{mitral}} \end{aligned} \tag{5.29}$$

where e is the system energy per unit mass, ρ the density of the blood, $\mathbf{v}$ is the absolute velocity, $\hat{\mathbf{n}}$ is the surface normal, φ_{mitral} is the mitral valve function and m is the mass of the inner volume of the left atrium. The system energy per unit mass is defined as the operator

$$\frac{dE}{dm} = e = e_{\text{kinetic}} + e_{\text{potential}} \tag{5.30}$$

where e_{kinetic} is the contribution from kinetic energy and $e_{\text{potential}}$ is the contribution from potential energy. The kinetic energy contains contributions from the pulmonary vein flow, the retained blood flow of inside of the left atrium and the outgoing blood through the mitral valve. The potential energy is stored in atrial vortices and in tissue during deformation.

The shaft work is mostly the work done in long axial direction in a piston-like fashion. The work is done by different mechanisms depending on the phase of the cardiac cycle. The time derivative of the work is given by

$$\frac{dW}{dt} = \dot{W}_{\text{shaft}} = \begin{cases} \dot{W}(t)_{\text{VC}} + \dot{W}(t)_{\text{ESE}} & t \in \text{systole} \\ \dot{W}(t)_{\text{ESE}} & t \in \text{diastole (fast filling phase)} \\ \dot{W}(t)_{\text{AC}} & t \in \text{diastole (slow filling phase)} \end{cases}$$

where $W(t)_{\text{VC}}$ is the work done by the myocardium during ventricular contraction, $W(t)_{\text{ESE}}$ is the work done by elastic strain energy and $W(t)_{\text{AC}}$ is the contribution from the atrial contraction.

5.5.2 Left ventricle

The left ventricle is modelled as a moving deformable control volume with one inlet, the mitral valve and one outlet, the aortic valve.

Mass conservation

The time derivative of the system mass is equal to the difference between change of internal mass over time and the mass flow trough the aorta and the mitral valve. The mass balance equation is given as

$$\begin{aligned}\frac{d}{dt}\left(m\right)_{\text{system}} =& \frac{d}{dt}\left(\int_{LV}\rho dV\right) + \int \rho\left(\mathbf{v}_{\text{r}}\cdot\hat{\mathbf{n}}\right)dA_{\text{aorta}} \\ &+ \varphi_{\text{mitral}}(t)\int \rho\left(\mathbf{v}_{\text{r}}\cdot\hat{\mathbf{n}}\right)dA_{\text{mitral}} = 0\end{aligned} \tag{5.31}$$

where m is the mass of the inner volume of the left ventricle, ρ the density of the blood, $\mathbf{v}_{\text{r}}$ is the relative velocity, $\hat{\mathbf{n}}$ is the surface normal and φ_{mitral} is the mitral valve function.

Linear momentum relation

The linear momentum relation answers to how energy will be distributed in the system. The change of linear momentum of the system over time is given by

$$\frac{d}{dt}\left(m\mathbf{v}\right)_{\text{system}} = \sum \mathbf{F} - \int_{\text{LV}} \mathbf{a}_{\text{r}} dm = 0 \tag{5.32}$$

where the first term on the right hand side is the sum of forces acting on the system and the second term is Newton's second law applied to a moving system with a relative acceleration, $\mathbf{a}_{\text{r}}$, which is given by

$$\mathbf{a}_{\text{r}} = \frac{d^2\mathbf{R}}{dt^2} + \frac{d\boldsymbol{\Omega}}{dt}\times\mathbf{r} \tag{5.33}$$

where the first term on the right hand side is the acceleration of the origin $\mathbf{R}$ of a relative coordinate system and the second term is the angular acceleration effect in eulerian coordinates and $\boldsymbol{\Omega}$ is absolute angular velocity.

The mass of the muscular wall can be seen as infinite since it is supported by the surrounding tissue [20]. By combining this and the assumption that the inner walls of the heart are streamlined, the losses of kinetic energy of the blood to the walls will be limited. By applying Reynolds Transport Theorem to linear momentum, the equation takes the form

$$\begin{aligned}\frac{d}{dt}\left(m\mathbf{v}\right)_{\text{system}} =& \frac{d}{dt}\left(\int_{\text{LV}}\mathbf{v}\rho dV\right) + \int \mathbf{v}\rho\left(\mathbf{v}_{r}\cdot\hat{\mathbf{n}}\right)dA_{\text{aorta}} \\ &+ \varphi_{\text{mitral}}(t)\int \mathbf{v}\rho\left(\mathbf{v}_{\text{r}}\cdot\hat{\mathbf{n}}\right)dA_{\text{mitral}}\end{aligned} \tag{5.34}$$

where m is the mass of the inner volume of the left ventricle, ρ the density of the blood, $\mathbf{v}$ is the absolute velocity, $\hat{\mathbf{n}}$ is the surface normal and φ_{mitral} is the mitral valve function.

Angular momentum relation

The angular momentum relation shows whether the control volume opposes a possible torque caused by the inflows/outflows or not. If the left ventricle would not oppose the torque, the whole volume would rotate. The angular momentum of the system is the

mass integral of the angular moments of every elemental mass dm within the system about an arbitrary point **P** . The angular moment is defined as

$$\mathbf{H}_P = \int_{\text{system}} (\mathbf{r} \times \mathbf{v})\, dm \tag{5.35}$$

where **r** is the distance between point **P** and the elemental mass dm. The change of angular momentum of the left ventricle over time is the torque and is given by

$$\frac{d\mathbf{H}_P}{dt} = \sum (\mathbf{r} \times \mathbf{F})_P - \int_{\text{LV}} (\mathbf{r} \times \mathbf{a}_{\text{r}})\, dm \tag{5.36}$$

where the first term on the right hand side is the sum of moments acting on the system and the second term is the relative torque based on Newton's second law applied to a moving system with a relative acceleration, $\mathbf{a}_{\text{r}}$.

By applying Reynolds Transport Theorem to angular momentum, the torque equation takes the form.

$$\begin{aligned}\frac{d\mathbf{H}_P}{dt} =& \frac{d}{dt}\left(\int_{\text{LV}} (\mathbf{r} \times \mathbf{v})\, \rho dV\right) + \int (\mathbf{r} \times \mathbf{v})\, \rho\, (\mathbf{v}_{\text{r}} \cdot \hat{\mathbf{n}})\, dA_{\text{aorta}} \\ &+ \varphi_{\text{mitral}}(t) \int (\mathbf{r} \times \mathbf{v})\, \rho\, (\mathbf{v}_{\text{r}} \cdot \hat{\mathbf{n}})\, dA_{\text{mitral}}\end{aligned} \tag{5.37}$$

where the first term on the right hand side is the moment that the control volume has to balance out the applied moments with, if the control volume should stay in its original position, the second term on the right hand side is the contribution of the aortic flow to a total moment about point **P** and the third term is the mitral contribution.

Energy equation

The time derivative of the applied work must balance the change of energy of the left ventricle in the following way

$$\frac{dQ}{dt} - \frac{dW}{dt} = \frac{dE}{dt} \tag{5.38}$$

where Q is heat, W is the applied work and E is the energy. In order to analyse energy relations with Reynolds Transport Theorem, the following equation is used

$$\begin{aligned}\frac{dE}{dt} =& \frac{d}{dt}\left(\int_{LV} e\rho dV\right) + \int e\rho\, (\mathbf{v} \cdot \hat{\mathbf{n}})\, dA_{\text{aorta}} \\ &+ \varphi_{\text{mitral}}(t) \int e\rho\, (\mathbf{v} \cdot \hat{\mathbf{n}})\, dA_{\text{mitral}}\end{aligned} \tag{5.39}$$

where e is the system energy per unit mass, ρ the density of the blood, $\mathbf{v}$ is the absolute velocity, $\hat{\mathbf{n}}$ is the surface normal, φ_{mitral} is the mitral valve function and m is the mass of the inner volume of the left ventricle. The system energy per unit mass is defined as the operator

$$\frac{dE}{dm} = e = e_{\text{kinetic}} + e_{\text{potential}} \tag{5.40}$$

where e_{kinetic} is the contribution from kinetic energy and $e_{\text{potential}}$ is the contribution from potential energy. The kinetic energy is the kinetic energy of the incoming blood, the outgoing blood to the aorta and the retained flow inside the left ventricle. The potential energy is the energy stored in ventricular vortices and in tissue during deformation. The shaft work is mostly the work done in long axial direction in a pistonlike fashion. The work is done by different mechanisms dependening on the phase of the cardiac cycle. The time derivative of the work is given by

$$\frac{dW}{dt} = \dot{W}_{\text{shaft}} = \begin{cases} \dot{W}(t)_{\text{VC}} + \dot{W}(t)_{\text{ESE}} & t \in \text{systole} \\ \dot{W}(t)_{\text{ESE}} & t \in \text{diastole (fast filling phase)} \\ \dot{W}(t)_{\text{AC}} & t \in \text{diastole (slow filling phase)} \end{cases}$$

where $W(t)_{\text{VC}}$ is the work done by the myocardium during ventricular contraction, $W(t)_{\text{ESE}}$ is the work done by elastic strain energy and $W(t)_{\text{AC}}$ is the contribution from the atrial contraction.

5.6 Flow and kinetic energy calculations

A Simulink model was built based on the mathematical model and the data acquired with MRI. The model makes it possible to balance flows and to investigate how the flows and corresponding kinetic energies in the pulmonary veins are related to the flow and kinetic energies over the mitral valve and in the aorta in every time step of the cardiac cycle. The outputs of the model are the AV-plane position over time, the left heart volume variation, the pulmonary vein flow, the mitral valve flow, the aortic flow, the incoming kinetic energy and the outgoing kinetic energy in the left atrium and the left ventricle.

Chapter 6

Results

In this chapter the results of the 3D-flow analysis, flow and energy calculations and the high cardiac measurements are presented.

6.1 3D-flow analysis

The 3D-flow MRI data acquisition was performed on the subjects at rest.

Pathlines for the four pulmonary veins (VPSS,VPSI, VPDS and VPDI) for the two subjects are presented in Figure 6.1. The VPSI path spirals several laps before it passes through the mitral valve. The VPSS path encircles old blood once and then goes in apical direction. The paths of the blood from VPDS and VPDI go along the atrial septal wall towards apex without any significant circulation. The streamline and curl plots of the left atrium are shown in Figure 6.2. There is no vortex at end diastole. The atrial vortex is most well defined by the curl in systole as the pulmonary vein flow reaches its peak. As the mitral valve opens, the circulating blood leaves its circular path and travels in the apical direction. The atrial vortex is rebuild during diastole and is most well defined just before the atrial contraction begins. Figure 6.3 shows how the incoming blood encapsulates old blood in the left atrium during systole. The mitral flow pathlines in Figure 6.4 show that the mitral flow originates mostly from the atrial vortex. The minor portion of the blood that can be derived from the previous cardiac cycle is visible as the intensive green behind VPSS in A and B. The blood in the vortex has a velocity of approximately 0.25 m/s in both subject A and subject B. The aortic flow pathlines in Figure 6.5-6.7 show that the contribution of direct flow to the aortic flow is present in both subjects in early systole and only subject A at the aortic flow peak in systole. There is no contribution from direct flow to the aortic flow in late systole in either subject. The disturbances in the area of the initial positions of the particles are caused by the movement of the AV-plane.

6.2 Flow and kinetic energy calculations

The displacement of the AV-plane of subject A and subject B are shown in Figure 6.8. The shapes of the curves are similar, but the amplitudes differ. The plateau in diastole should be noted. The left heart volume variation of subject A and subject B are shown in Figure 6.9. The amplitudes are almost identical, but the volume change during atrial

contraction is larger in subject A. Figure 6.10 and Figure 6.11 show the flows in the left heart of subject A and subject B respectively. The pulmonary vein flows are biphasic in both subjects. The mitral flow of subject A is left out due to technical problems. The mitral flow of subject B is biphasic. Small aortic flows can be observed during diastole that are caused by the movement of the AV-plane.

The kinetic energy of the flows of subject A and subject B are shown in Figure 6.12 and 6.13. In subject A, 46% of the total kinetic energy of the pulmonary vein flow has passed into the left atrium at end systole compared to 55% in subject B. The accumulated kinetic energy of the pulmonary vein flows corresponds to 17% of the accumulated kinetic energy of the aortic flow in subject A compared to 18% in subject B. The accumulated kinetic energy of the mitral flow of subject B from start diastole to the start of the atrial contraction corresponds to 66% of the kinetic energy of the pulmonary vein flows. The atrial contraction could contribute with 10% to the accumulated kinetic energy of the mitral flow at most. The average heart rate of subject A was 61 bpm (56 bpm - 63 bpm) during flow MRI. The average heart rate of subject B was 56 bpm (52 bpm - 61 bpm) during flow MRI. The heart rates of subject B during cine MRI were four-chamber: 52 bpm, two-chamber: 52 bpm and LVOT 55 bpm.

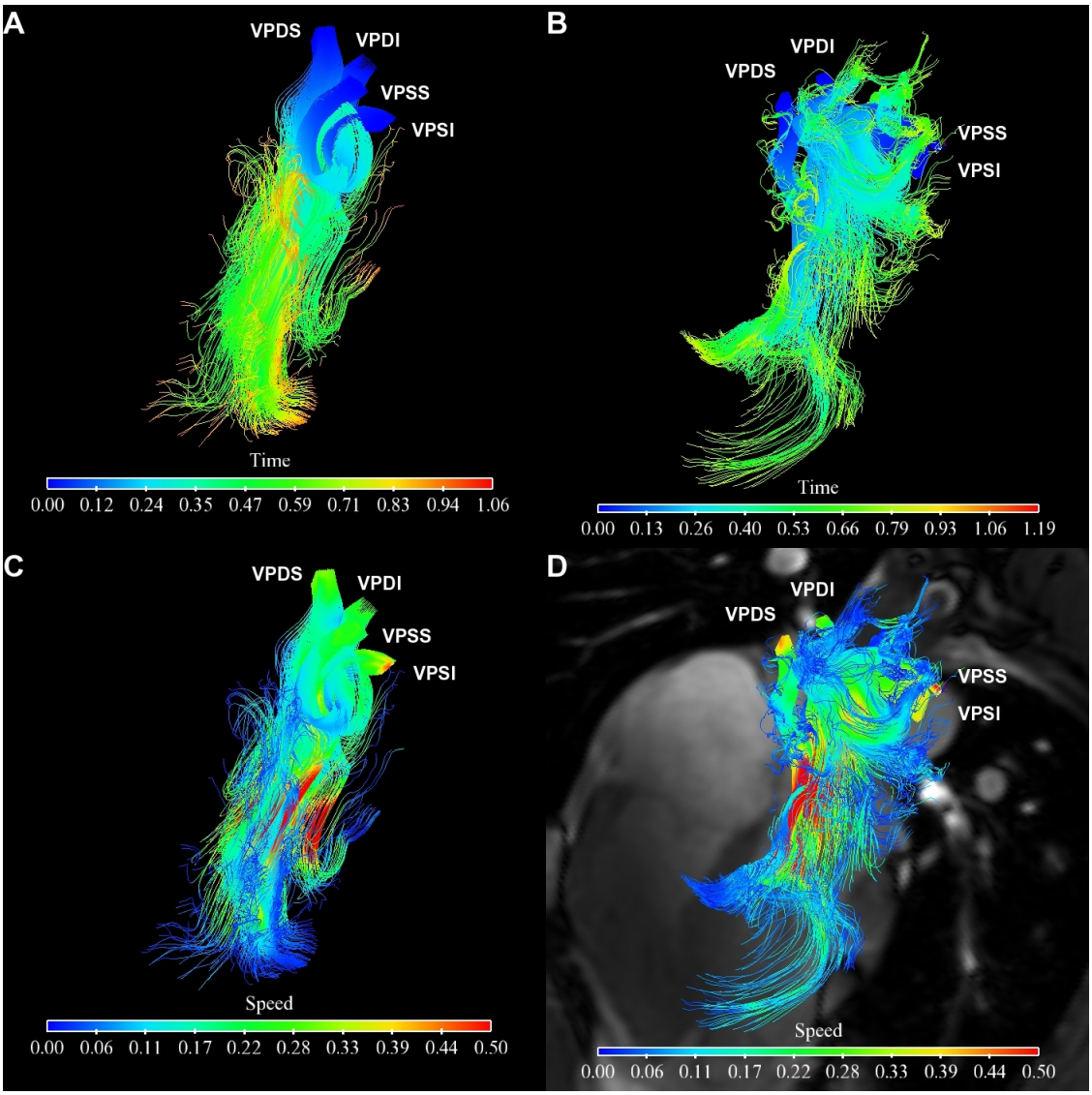

Figure 6.1: The two left panels show pulmonary vein flow pathlines of subject A and the two right panels of subject B. The particles are released at the time of the systolic flow peak. The pathlines stop at the end of the current cardiac cycle. Panels A and B show the pathlines of subject A and subject B colored by time. Panels C and D are the corresponding pathlines colored by speed. The VPSI path spirals several laps before it passes through the mitral valve. The VPSS path encircles old blood once and then goes in apical direction. The paths of the blood from VPDS and VPDI go along the atrial septal wall towards apex without any significant circulation. Speed in [m/s] and time in [s].

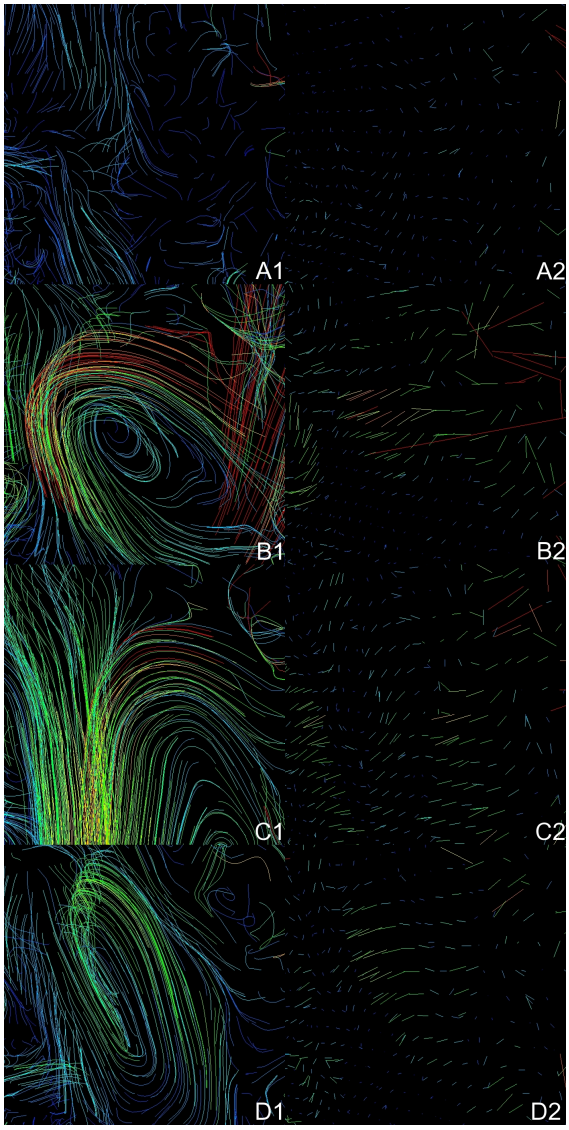

Figure 6.2: The left hand panels (1) are curvlinear streamline plots and the right hand panels (2) are the corresponding curl plots. Row A is at end diastole, row B is at the pulmonary flow peak in systole, row C is at the mitral flow peak in diastole and row D is at mid diastole. The plane is perpendicular to the axis of the systolic VPSI flow in the left atrium of subject A. There is no vortex at A. B and D are the two occasions when the atrial vortex is largest and most well defined by the curl. At D, the axis of rotation has turned a couple of degrees clockwise relative the axis of rotation in B. The open mitral valve lets the blood of the vortex leave the circular path in C and travel in apical direction.

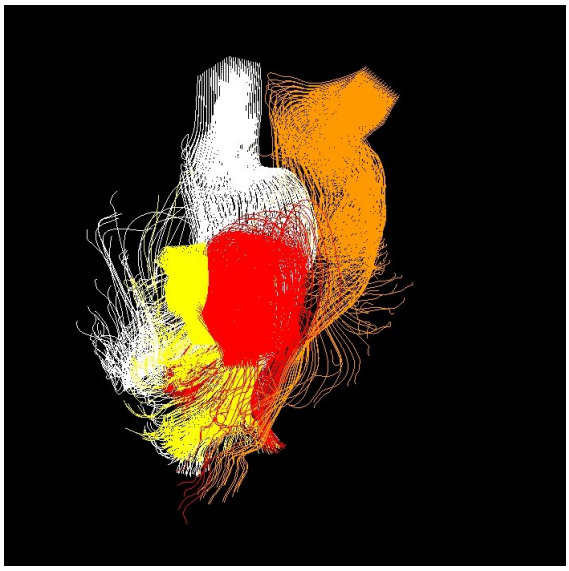

Figure 6.3: The pulmonary vein flows in the left atrium of subject A encapsulate blood from the previous cardiac cycle and pass on kinetic energy. VPSI - yellow, VPSS - red, VPDI - orange and VPDS - white.

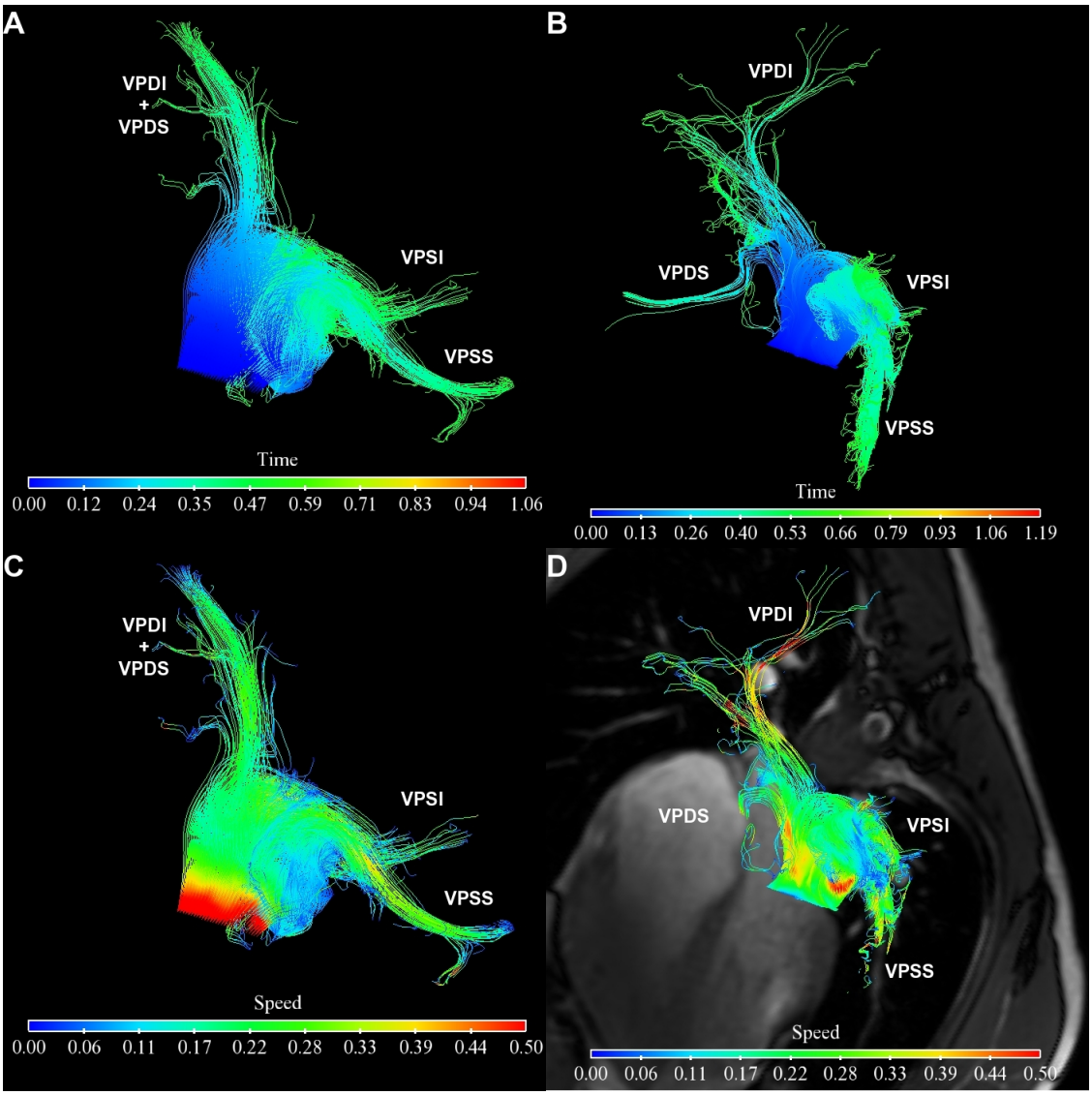

Figure 6.4: The two left panels show mitral flow pathlines backwards in time of subject A and the two right panels of subject B. The particles are released at the time of the first diastolic flow peak. The pathlines stop at the start of the current cardiac cycle. In panel A and panel B, the pathlines of subject A and subject B are colored by time. Panels C and D are the corresponding pathlines colored by speed. The mitral flow originates mostly from an atrial vortex. The minor portion of blood that can be derived from the previous cardiac cycle is visible as the intensive green behind VPSS in panel A and panel B. The blood in the vortex has a velocity of approximately 0.25m/s in both subject A and subject B. Speed in [m/s] and time in [s].

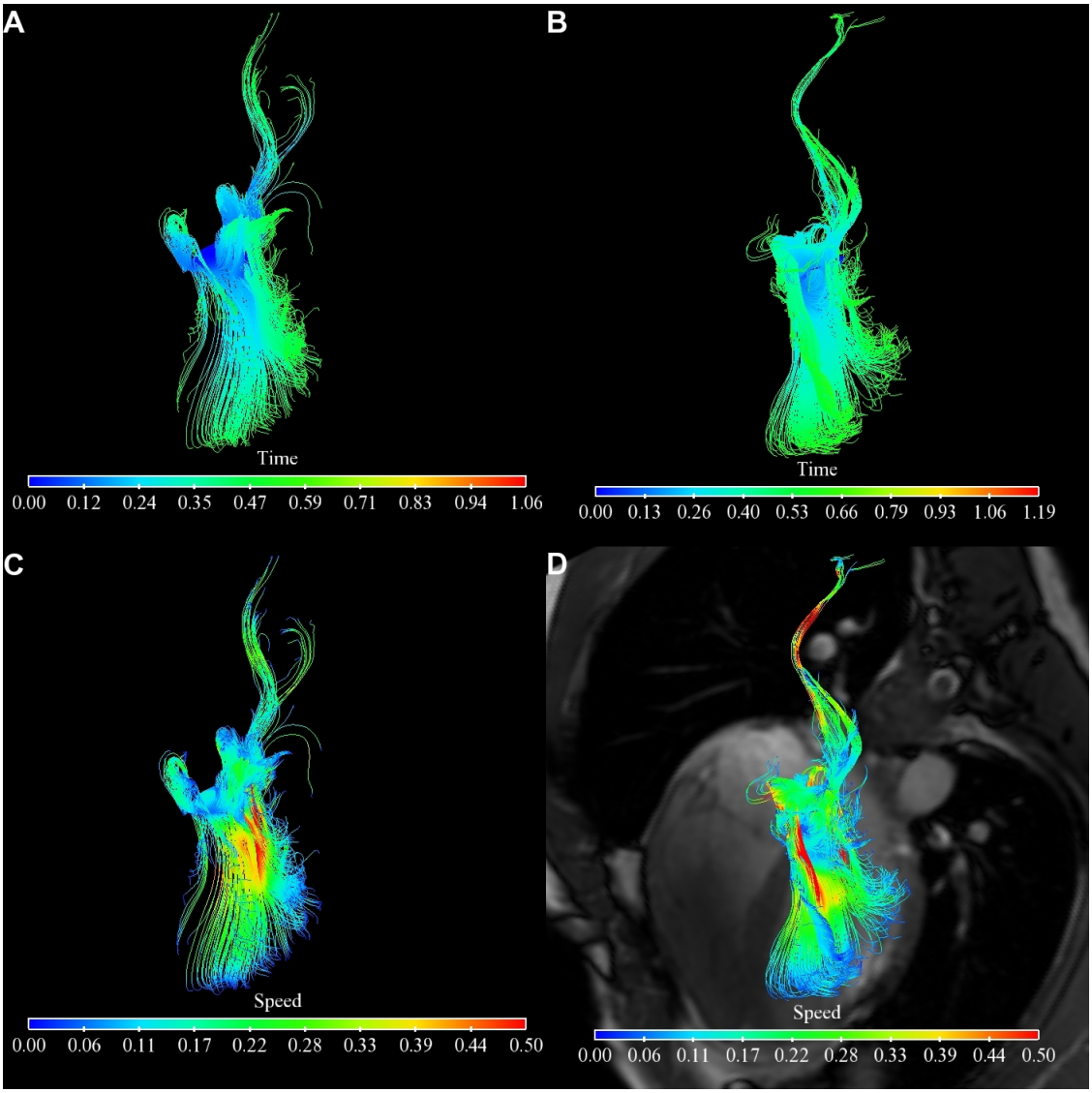

Figure 6.5: The two left panels show aortic flow pathlines backward in time of subject A and the two right panels of subject B. The particles are released in early systole. The pathlines stop at the start of the current cardiac cycle. In panel A and panel B, the pathlines of subject A and subject B are colored by time. Panels C and D are the corresponding pathlines colored by speed. Direct flow is visible in both of the subjects. Speed in [m/s] and time in [s].

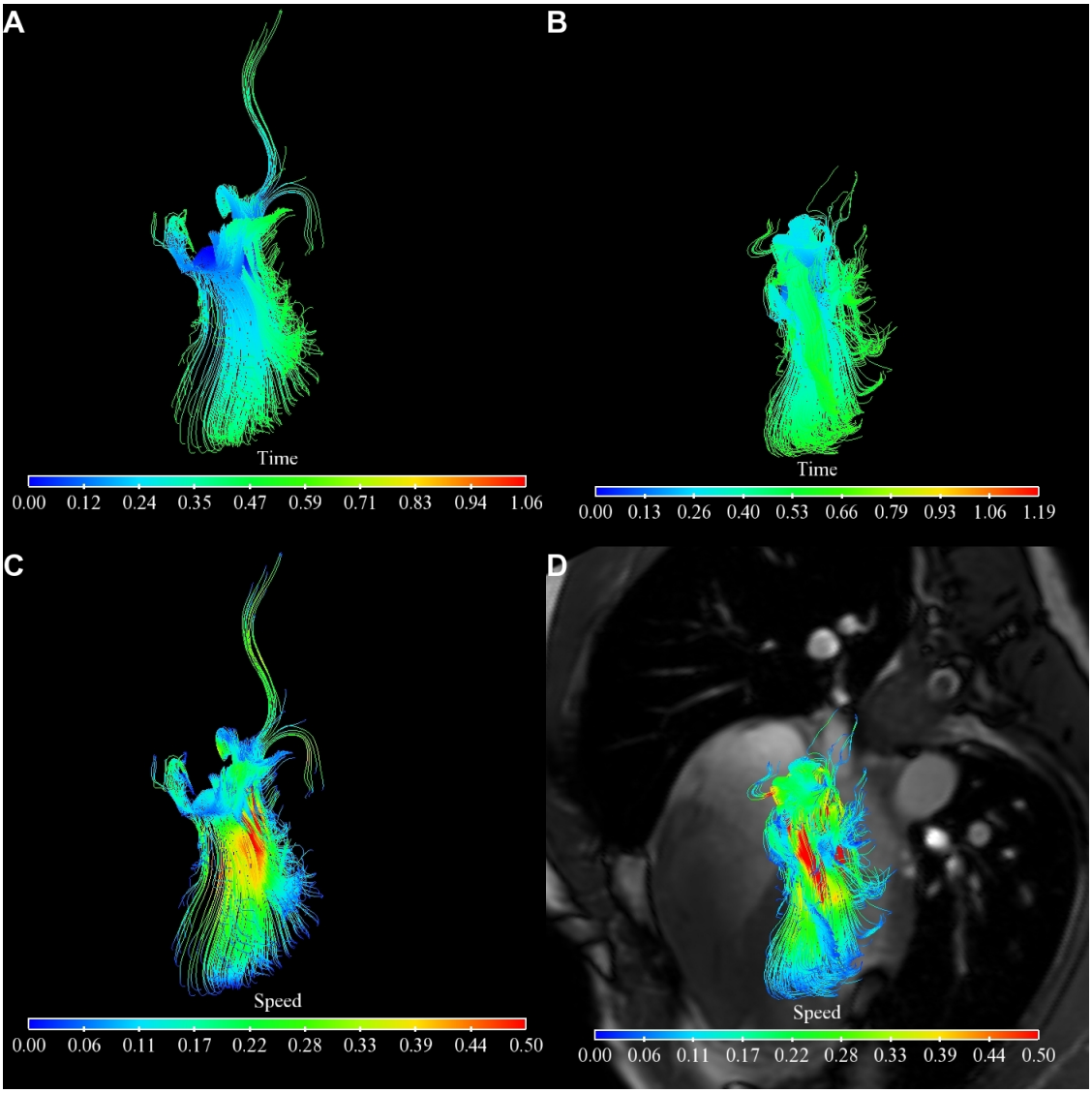

Figure 6.6: The two left panels show aortic flow pathlines backward in time of subject A and the two right panels of subject B. The particles are released at the time of the systolic flow peak. The pathlines stop at the start of the current cardiac cycle. In panel A and panel B, the pathlines of subject A and subject B are colored as timelines. Panels C and D are the corresponding pathlines colored by speed. Direct flow is only visible in subject A. Speed in [m/s] and time in [s].

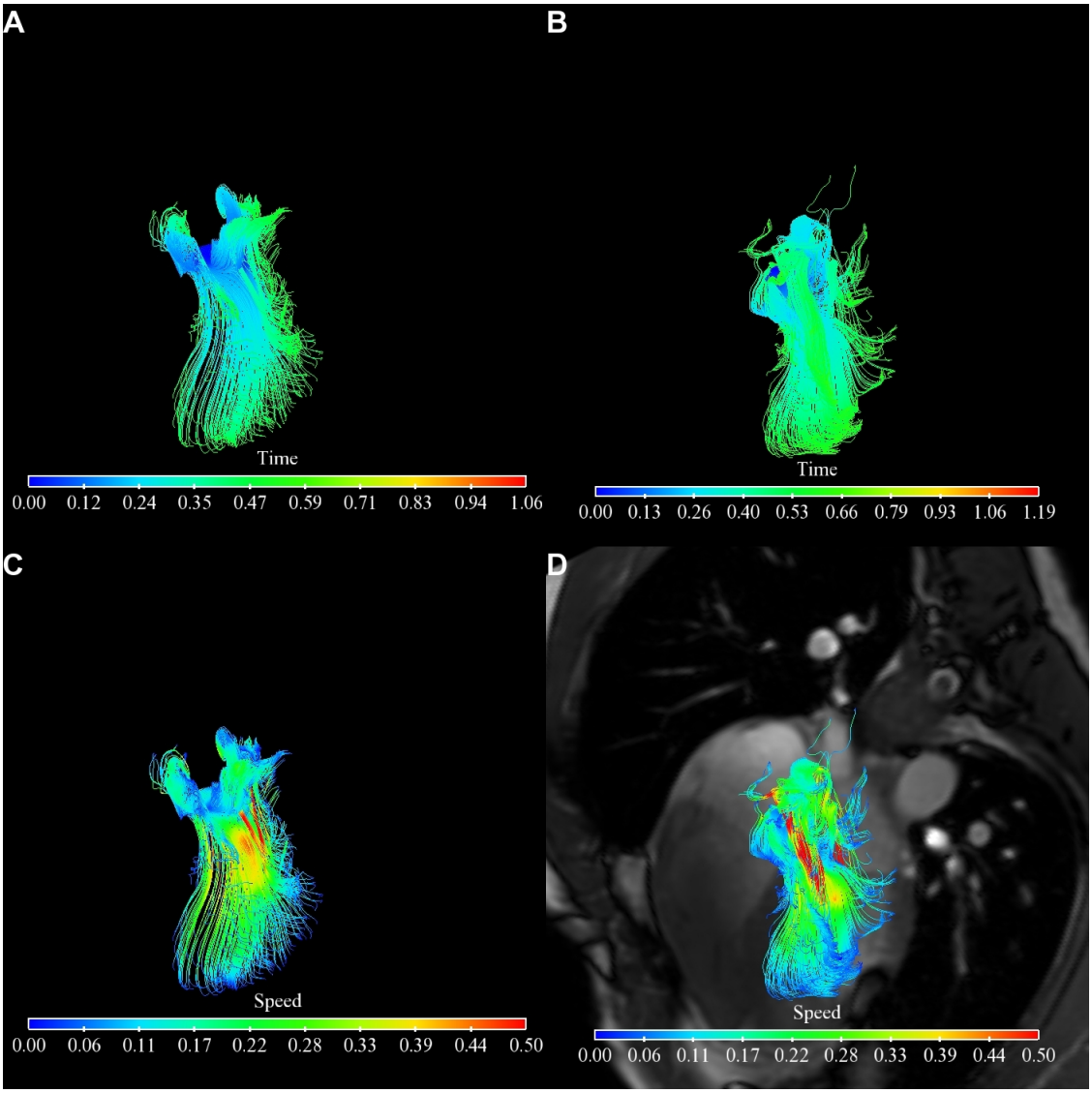

Figure 6.7: The two left panels show aortic flow pathlines backward in time of subject A and the two right panels of subject B. The particles are released in late systole. The pathlines stop at the start of the current cardiac cycle. In panel A and panel B, the pathlines of subject A and subject B are colored as timelines. Panels C and D are the corresponding pathlines colored in speed. Speed in [m/s] and time in [s].

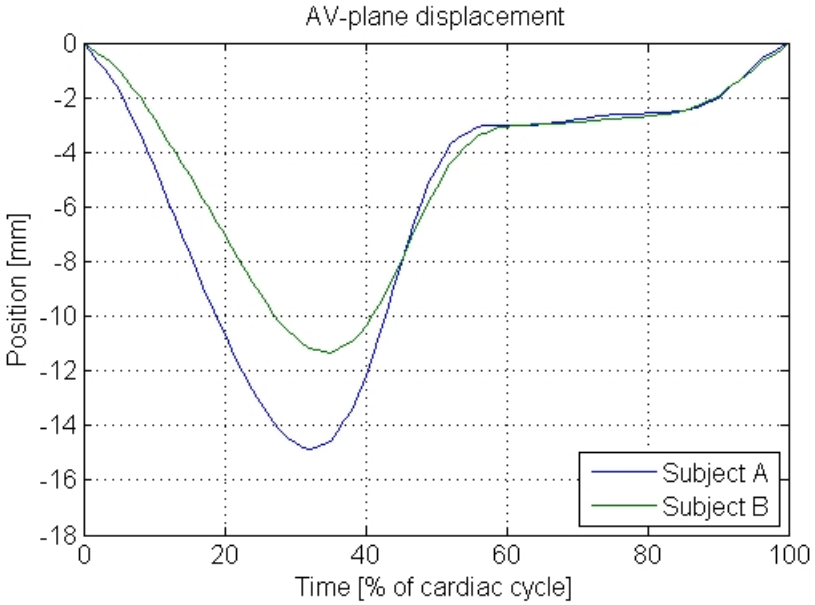

Figure 6.8: The displacement of the atrio-ventricular plane. The position is used when the mitral flow measurements are interpolated. Compare to Equation A.2 and Figure A.2.

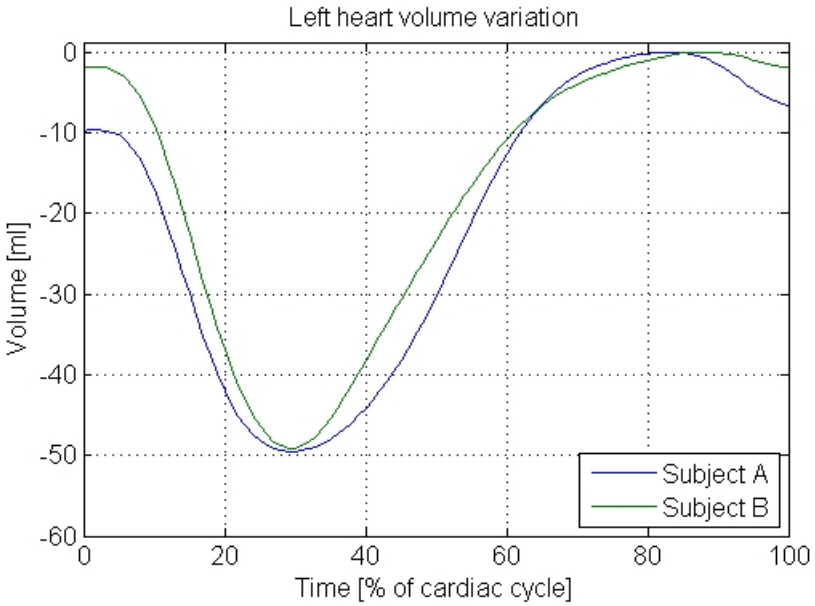

Figure 6.9: The left heart volume variation as given in Equation 5.12.

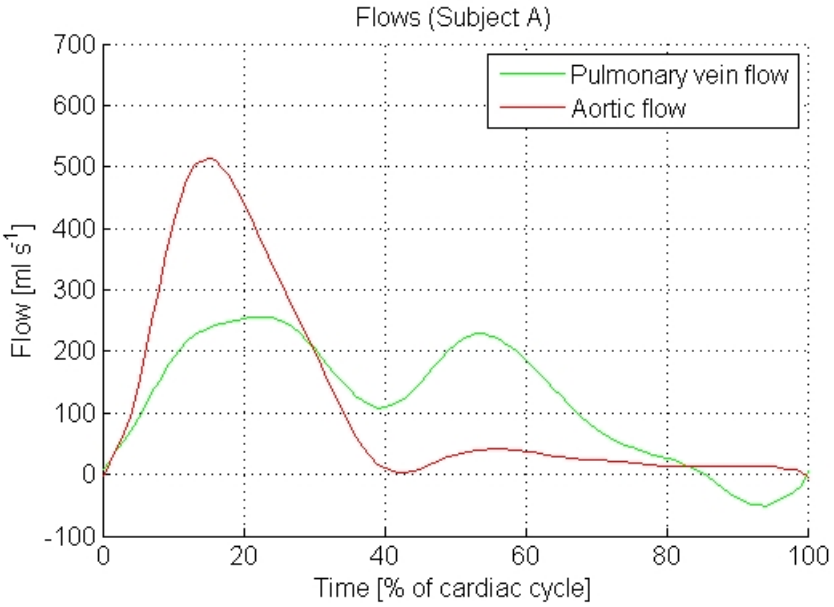

Figure 6.10: The incoming/outgoing flows in the left heart of subject A.

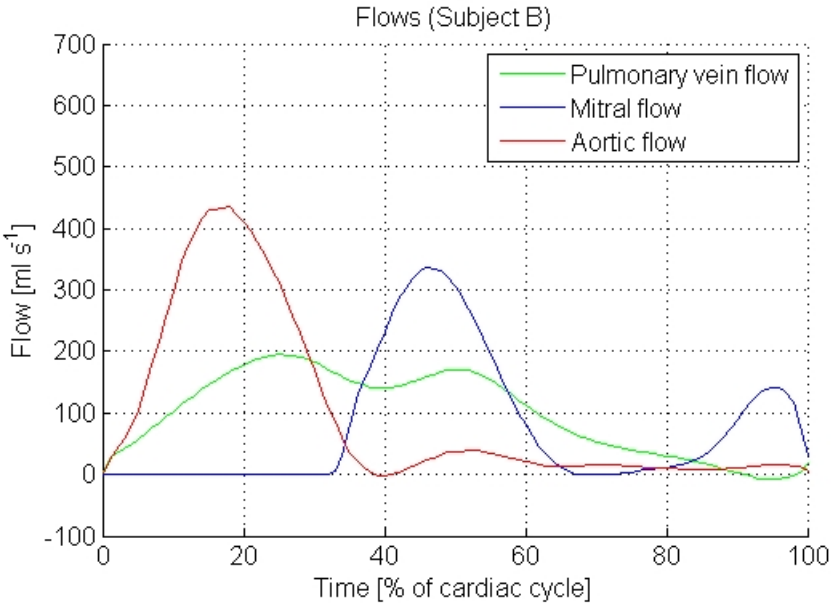

Figure 6.11: The incoming/outgoing flows in the left atrium and left ventricle of subject B.

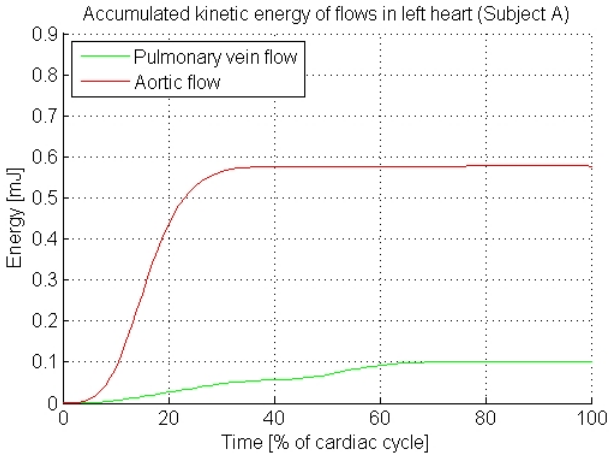

Figure 6.12: The accumulated kinetic energy of the incoming/outgoing flows in the left heart of subject A. The plots are the time integrals of the pulmonary vein flow and aortic flow kinetic energy contributions described in Equation 5.29 and 5.39. The final value is the kinetic energy content of the flow passing through the control surface every beat. 46% of the total kinetic energy of the pulmonary vein flow has passed into the left atrium at end systole. The accumulated kinetic energy of the pulmonary vein flows corresponds to 17% of the accumulated kinetic energy of the aortic flow.

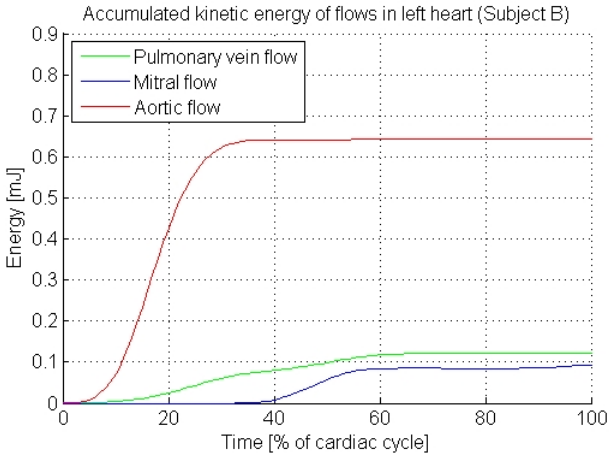

Figure 6.13: The accumulated kinetic energy of the incoming/outgoing flows in the left atrium and left ventricle of subject B. The plots are the time integrals of the pulmonary vein flow, mitral flow and aortic flow kinetic energy contributions described in Equation 5.29 and 5.39. The final value is the kinetic energy content of the flow passing through the control surface every beat. 55% of the energy of the pulmonary vein flow has passed into the left atrium at end systole. The accumulated kinetic energy of the mitral flow from start diastole to the start of the atrial contraction corresponds to 66% of the kinetic energy of the pulmonary vein flows. The atrial contraction could contribute with 10% to the accumulated kinetic energy of the mitral flow at most. The accumulated kinetic energy of the pulmonary vein flows corresponds to 18% of the accumulated kinetic energy of the aortic flow.

6.3 High cardiac output

The aortic flow of subject B at rest and during exercise are presented in Figure 6.14. The heart rate was 55 bpm at rest and 91 bpm during work. The cardiac output increased from 5.2 L/min to 9.4 L/min which corresponds to a 81% increase. The stroke volume increased from 94 ml to 103 ml. Flow kinetic energy content/beat during work: 0.23 mJ and at rest: 0.24 mJ. Flow kinetic energy content/minute during work: 21 mJ and at rest: 13 mJ. The increase of kinetic energy content per minute of the aortic flow was 62%. The duration of systole decreased with 13% and the duration of diastole decreased with 56% during work. The ratio between systole and diastole in the cardiac cycle is 44:56 at rest and 61:39 during work.

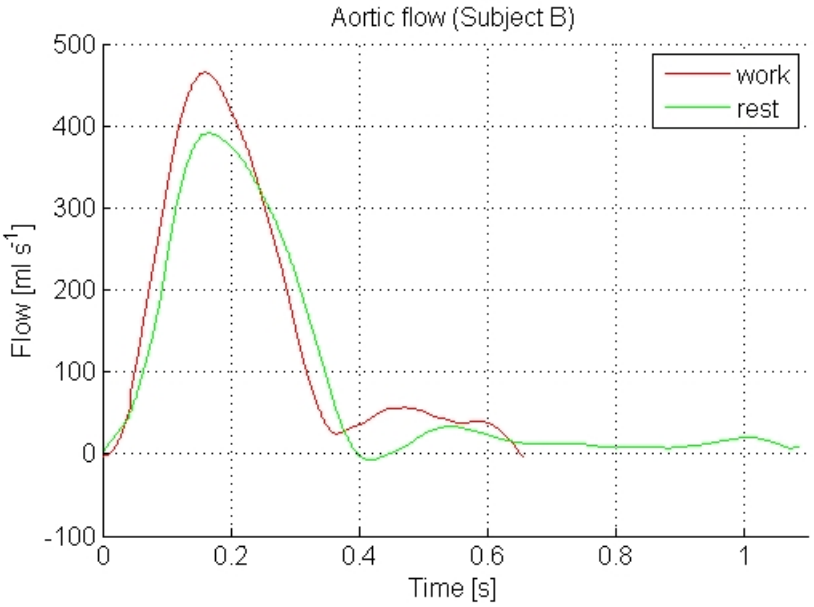

Figure 6.14: The aortic flow of subject B at rest and during physical work. The results are the average of five cardiac cycles in the rest case and six cardiac cycles in the work case using real time flow MRI. The heart rate was 55 bpm at rest and 91 bpm during work. The cardiac output increased from 5.2 L/min to 9.4 L/min which corresponds to a 81% increase. The stroke volume increased from 94 ml to 103 ml. Flow kinetic energy content/beat during work: 0.23 mJ and at rest: 0.24 mJ. Flow kinetic energy content/minute during work: 21 mJ and at rest: 13 mJ. The increase of kinetic energy content per minute of the aortic flow was 62%. The duration of systole decreased with 13% and the duration of diastole decreased with 56% during work. The ratio between systole and diastole in the cardiac cycle is 44:56 at rest and 61:39 during work.

Chapter 7

Discussion

This chapter presents the interpretation of the results, the limitations involved in the work, the conclusions that can be drawn and ideas for future work.

7.1 Interpretation

In this section, the results are put into context and theories are drawn up based on the results of this study and previous findings by others. The theories are to a large extent evidence based. The purpose of the theories is not to explain the function of the heart but a model of the heart.

7.1.1 3D-flow analysis

The pulmonary vein flow pathlines show that the paths of the incoming blood in the left atrium encapsulate the blood left from the previous cardiac cycle and kinetic energy of the new blood is passed on to the old blood, see Figure 6.1 and 6.3. This interaction causes the build up of an atrial vortex with an axis perpendicular to the AV-plane (Figure 6.4, 6.2 and [8]). In the same pathline plot, parts of the vortex ring below the mitral valve, shown by Heiberg *et al* [11], is visible in Figure 6.1. The vortex ring is a result of boundary layer separation between the retained ejection flow that travels along the inner walls of the left ventricle in basal direction and the incoming flow moving in apical direction. The combined shape of the mitral valve and the left ventricle is similar to a diffuser which also contributes to backflow if the boundary layers are thick [30]. The vortex ring may assist to create a passage for the direct ventricular inflow towards the aortic trunk and to stabilize the mitral leaflets.

The atrial contraction is responsible of generating the major portion of direct flow through the left ventricle [2]. This is indicated by the presence of the atrial contribution to the aortic flow shown in Figure 6.5. The atrial contraction does also give rise to the pulmonary vein back flow, see Figure 6.2, 6.10, 6.11 and 7.6. The direct flow to the aorta through the left ventricle comes from the right pulmonary veins and the atrial vortex. The retained ventricular flow dominates the aortic flow, which is consistent with the results of Bolger *et al* [2].

The atrial vortex is built up twice, once in systole and once in diastole. The rotating flow changes path as the mitral valve opens and goes towards apex due to centripetal

forces. After the first mitral flow peak, the vortex is reestablished, see Figure 6.2 and 7.1-7.6.

The mutual positions of the atrial inlets, the mitral valve leaflets and the aortic trunk creates an energy efficient asymmetric flow structure (Figure 7.1-7.6), which is similar to the one proposed earlier [16, 17]. The angles between the inlets/outlets and the inner walls of the left heart are arranged in a way that makes the flows coincide with vortices and/or inner walls in order to prevent losses in kinetic energy due to opposing flows or collisions with walls, see Figure 6.1 and 6.4.

The vortex patterns in the left heart seem to contribute more to dynamic paths of the blood than to changes of heart shape. Boundary layer separation limits opposing flows. The speed of the blood that is approaching the aortic trunk is approximately 0.2-0.3 m/s during diastole. This can be compared to a AV-plane velocity maximum of 0.15 m/s, which occurs in the fast filling phase. This indicates that the kinetic of the blood will contribute to the return of the AV-plane since the aortic valve is closed during this phase, see Figure 6.8, 6.5, 6.6 and 6.7. Kinetic energy is economized by directing the flow of blood towards the aortic trunk in order to minimize the length of the path and simultaneously make it approach obstacles from angles that minimize losses in linear momentum. The combined function of the flows reduces the risk of turbulence, which would increase the viscous friction if present.

The velocity of the blood that has passed the aortic valve seems to be too low since the average velocity at the aortic cross section at the flow peak is 0.6 m/s according to the flow MRI measurement, see Figure 6.6 and 6.10.

7.1.2 Flow and kinetic energy calculations

The energy calculations of the heart of subject B indicates that 68% of the incoming kinetic energy to the left atrium can be conserved in the atrial vortex for later use. The atrial contraction does only contribute with 10% to the kinetic energy of the mitral flow at most.

The total mitral flow measured is about 22% lower than the aortic flow and the pulmonary vein flow, which is close to the mitral annular excursion volume of 19% described by Carlhäll *et al* [3].

The interpretation of flow, volume variation and AV-plane displacement is found in Section 7.1.3. A study of 5-10 subjects would be needed for a physiological interpretation of the results.

The left heart volume variations of approximately 50ml shown in Figure 6.9 corresponds well to the results of Carlsson *et al* [4].

7.1.3 Cardiac cycle

The cardiac cycle has no beginning and no end, but for convenience, we can think of start systole as the starting point. The left atrial volume is minimal and no vortex is present at this time, see Figure 6.2 and 6.9. The ventricular isovolumetric contraction makes the ventricular pressure to exceed the arterial pressure and the aortic valve opens. The ventricular torsion takes place as the ventricular contraction starts to pull the AV-plan in apical direction.

The AV-plane movement in apical direction pushes a column of blood against the pressure load out through the aorta and causes a rise in left atrial volume, see Figure 7.1. This opens a volume for the blood of the pulmonary veins to fill. This suction

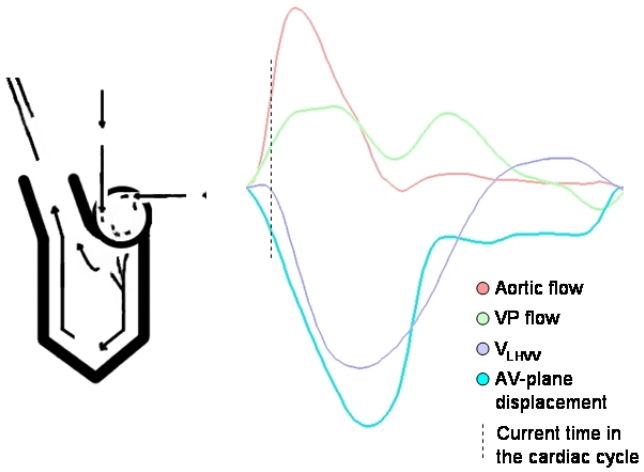

Figure 7.1: Early systole. The aortic valve is open and the mitral valve is closed. The ventricular contraction has started, the AV-plane is pulled towards apex and the movement causes suction in the left atrium and increases the kinetic energy of the blood in the left ventricle. The pulmonary vein flows encapsulate blood from previous cardiac cycles in the left atrium and starts the build up of an atrial vortex. The direct flow, which depends mainly on the atrial contraction, finds a way out to the aorta. The ventricular torsion takes place.

of blood is visible as the systolic pulmonary vein flow peak, see Figure 6.10 and 6.11. The movement of the AV-plane towards apex is not opposed by any significant spring forces in the left atrium since the auricles are unfolded [20]. The large arteries that are attached to the AV-plane, the aorta and the pulmonary artery, will store elastic energy when deformed [28]. The ventricular muscular wall thickens as the AV-plane is pulled towards apex (Figure 7.2 and [20]). The ventricular contraction has a radial component that causes the left heart volume decrease [5].

The ventricular muscular wall do work on itself as the collagen surrounding and interconnecting the myocytes stores elastic energy when the ventricle is twisted, deformed radially and axially [13]. The tissue surrounding the heart inside of thorax is deformed as the heart is deformed which gives rise to small pressure differences in thorax.

When the AV-plane has reached its bottom position, the aortic valve closes as the arterial pressure exceeds the static and dynamic ventricular pressure. At this point, the left heart volume reaches its minimum, see Figure 7.3 and 7.4.

Diastole starts, the isovolumetric relaxation follows and the mitral valve opens. As the isovolumetric relaxation is finished, the torsion component of the ventricular deformation recoils [13]. The AV-plane is pulled basally by the elastic strain energy of the large arteries and the ventricular wall and by the energy of the retained ejection flow, which in turn receives energy from the ventricular inflow, see Figure 7.4. The AV-plane movement redefines the border between the left atrium and the left ventricle.

The return of the AV-plane during the fast filling phase is even faster than the systolic

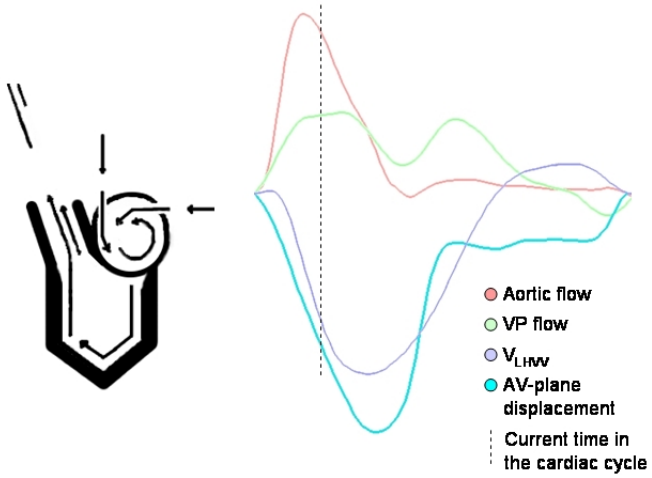

Figure 7.2: Mid systole. The aortic valve is open and the mitral valve is closed. The systolic pulmonary vein flow peak. The muscular wall thickens as the AV-plane is pulled in apical direction. The aortic flow is dominated by the retained ejection flow of the previous cardiac cycle.

ejection since no work has to be done against any pressure load except for the movement of the aorta and the pulmonary artery which can be observed as the two peaks in the aortic flow curve in diastole and also as the disturbances in the aortic flow pathlines, see Figure 6.10, 6.11 and 6.6. Consequently, the return of the AV-plane contributes to the pumping of the already ejected volume. This is visible as the diastolic increase in arterial pressure in Figure 4.2. The diastolic dip in the aortic flow curves visible in Figure 6.10, 6.11 and 7.4 is the return of the systolic ventricular pressure wave which is reflected in the large arteries. It coincides with the start of the return of the AV-plane. The period of the reflex seem to be about one fourth of the cardiac period, which agrees with the theories of destructive interference at higher frequencies in the artery tree proposed by Stergiopulos *et al* [27]. If the arteries would be stiffer, the reflex in the arteries might hit the AV-plane at a less advantageous position instead. This could lead a small loss of kinetic energy, which would make the return of the AV-plane more dependent on atrial contraction. The restoration of the radial shape of the left heart starts during the fast filling phase. It might not be obvious that the pumping of the heart also includes the total heart volume variation which indirectly affects the vessels inside of thorax, especially the lungs, the vena cavas and the pulmonary veins that have relatively low pressures. The radial ventricular force components caused by elastic strain energy and the recoil of the surrounding tissue will give rise to a slight increased pressure difference between the pulmonary veins and left heart, compare to Equation 5.11. The lungs are affected by cardiogenic oscillations that cause a change of pharyngoesophageal segment (PES) pressure that has a pattern similar to an inverted left heart volume variation curve. A useful comparison between the cardiac cycle and PES pressure is shown by Lischtwarck-Aschoff *et al* [19]. The total heart volume variation causes the

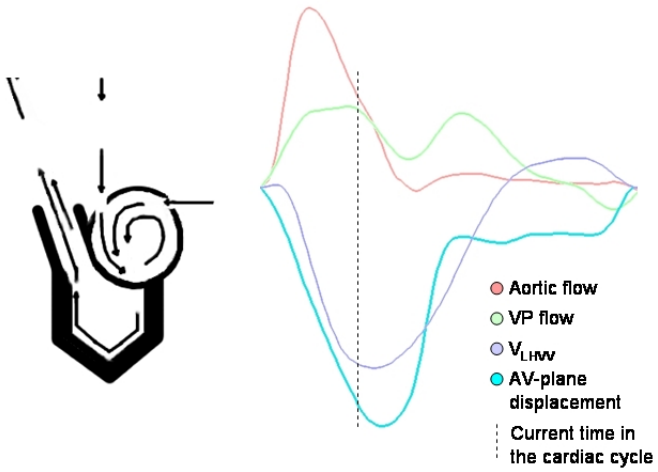

Figure 7.3: Late systole. The aortic valve is open and the mitral valve is closed. The left heart is about to reach its minimum volume. The AV-plane is almost at its most apical position. The aortic flow is dominated by the retained ejection flow of the previous cardiac cycle.

diastolic pulmonary vein flow peak which coincides with the first mitral flow peak and the diastolic AV-plane plateau. The diastolic atrial vortex is present during the duration of the plateau, see Figure 6.2. All together, the main factors that restores the shape of the heart are internal elastic energy and the striving of cancelling out potential pressure differences between the heart and the veins and between the heart and its surroundings in thorax. Compare with Equation 5.11. The fast filling phase ends when the AV-plane comes close to its equilibrium point, see Figure 6.8 and 7.5. The left heart volume continues to increase until the atria contract and pertubates the system.

The starting point of the atrial contraction is the occasion when the heart has been able to restore the state of lowest potential energy possible. The atrial contraction pulls the AV-plane even more basally and squeezes out the last portion of the atrial vortex, see Figure 7.6. Elastic energy is stored to a certain extent in the titin/connectin proteins of the muscle fibres as the muscles are streched out [7, 9, 18]. The elastic energy will be useful in the start of the AV-plane movement in apical direction in early systole. The AV-plane curve can be compared to the length of a one-dimensional spring that is extended by atrial contraction and then compressed by ventricular contraction. All muscles are relaxed during the fast filling phase in diastole which makes it similar to the restoration towards the equilibrium length of a spring.

7.1.4 Function of ventricular septum

Ventricular septum can be regarded as a mechanical low pass filter that reduces the impact of the inspiration on pressure variation in the vascular system by using the striving of the nature to increase entropy. Compare with Equation 5.11. During inspiration, the filling volume of the left heart increases. The inhaled air occupies a volume in thorax,

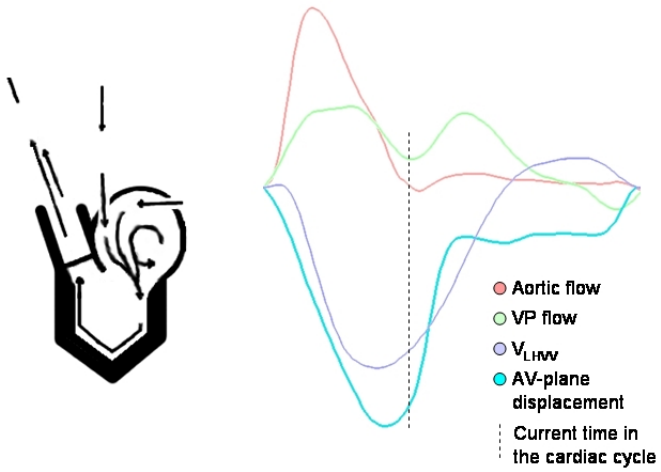

Figure 7.4: Early diastole. The aortic valve is closed and the mitral valve is open. All muscles are relaxed and the isovolumetric relaxation has just ended. The fast filling phase starts, which lets the left heart volume to increase and the return of the AV-plane to begin. The torsion recoil takes place and restores the angular relation between the basal and apical muscular wall of the left ventricle. The elastic strain energy starts to move the AV-plane in basal direction. The retained inflow goes along the lateral ventricular wall towards apex in order to fill the volume that the retained ejection flow leaves. Kinetic energy of the retained ejection flow and retained inflow contributes to the AV-plane return. The arterial pressure wave reflex reaches the AV-plane.

partly a volume stolen from the pulmonary veins that have to deliver an extra amount of blood to the left atrium. The increase in left heart end diastolic volume will be compensated with a decrease in right heart end diastolic volume since the ventricular septum works as a membrane during diastole when the myocardium is relaxed [20]. During the next cardiac cycle, the left heart end diastolic volume will be slightly smaller than ordinary since the incoming blood is related to the stroke volume of the right heart in the previous cardiac cycle.

7.1.5 Driven pendulum

In our high cardiac output experiment it seems as if the arterial reflex reaches the AV-plane during its way towards apex, but in rest, it reaches the AV-plane just as it is about to start its return. The reflexes are likely synchronized with the pumping movements or cancelled out due to destructive interference at high cardiac output. The fast filling phase is followed almost directly by atrial contraction which explains how diastole can be shortened by changing the delay between ventricular relaxation and atrial contraction at increased cardiac output, see Figure 6.14. When the heart delivers even greater volumes, the fast filling phase and the atrial contraction will create a seamless return of the AV-plane. The heart will switch into a new working mode and the AV-plane displacement curve will get a sinusoidal pattern, which is shown by Kilner *et al* [15].

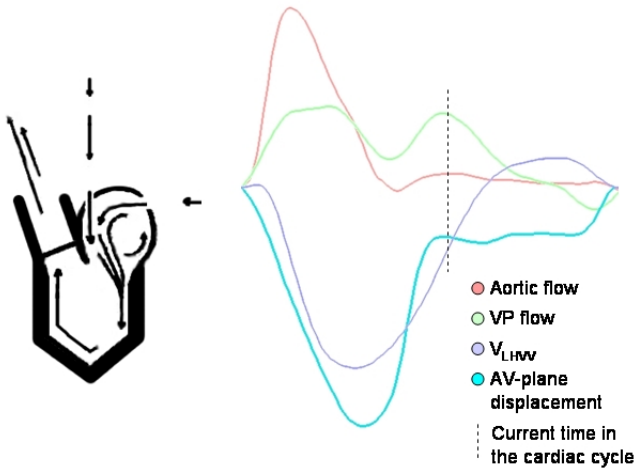

Figure 7.5: Mid diastole. The aortic valve is closed and the mitral valve is open. The fast filling phase ends. The AV-plane is close to its equilibrium position. The left heart volume increases as the shape of the heart goes towards its low energy state. The increase of left heart volume causes suction in the left atrium. There is a diastolic aortic flow peak due to the movement of the AV-plane.

The heart becomes a driven pendulum working at its natural frequency which will minimize energy cost. A technical model is presented in Figure 7.7. The mitral valve is slightly open during systole and the aortic valve during diastole, which is shown by the flows measured by Kilner *et al* [15]. The AV-plane will still work as a piston. The only difference is that the dynamic function of the soft leaflets will create a gradual narrowing similar to a cone. The flowing blood will accelerate as it approaches the valve opening. The local pressure difference will decide how large the aperture can be and still make sure that no back flow is allowed. In other words, the aperture is controlled by the static and dynamic pressure. The blood passing through the valve is a part of the piston when it is located in the theoretical piston surface. The heart rate can be increased by adjusting the stroke length. The retained ejection flow and the retained inflow can be considered as the major portion of the mass of the pendulum. This mass is controlled by the valves and can be reduced by increasing the direct flow. The direct flow should be thought of as a bypassed volume that lets superfluous kinetic energy out through the aorta without being involved in the pumping mechanics. At high cardiac output, the retained ejection flow and retained inflow can be reduced in size since the kinetic energy is proportional to the squared velocity. A smaller volume of blood is then needed in order to supply the AV-plane with necessary energy. The aortic valve lets out all of the flow that is not needed for the return, which will conserve the kinetic energy of the blood more efficient. Consequently, the relative and quantitative portion of direct inflow will increase. The function of the valves can also be seen as security vents that protect the tissue from being damaged due to harmful extension.

The total heart volume variation will be smaller during exercise since the restoration

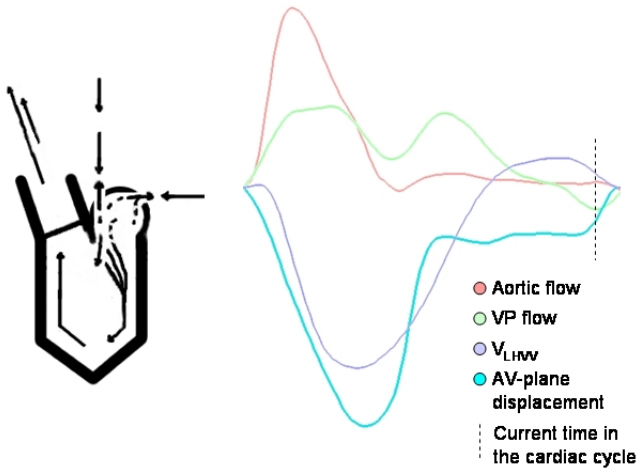

Figure 7.6: Late diastole. The aortic valve is closed and the mitral valve is open. The atrial contraction pulls the AV-plane in basal direction and makes the left heart volume to decrease. There is a slight increase in aortic flow due to the movement of the AV-plane.

of shape is slow and continues after the fast filling phase has ended until the atrial contraction is initiated at rest, see Figure 7.1. By reducing the radial change of shape, less energy will be lost to the surroundings [20]. The contribution from the left heart volume variation to the diastolic pulmonary vein flow will be rather insignificant compared to the contributions from the skeletal muscle pump and inspiration. Reduced left heart volume variation at high cardiac output has been proposed by Carlsson *et al* [5].

At high cardiac output, the velocities in the heart will be higher which could cause increased boundary layer separation that isolates opposing flows from each other.

7.2 Limitations

The MRI technique used is limited to measurements in supine position, which makes the results of the measurements trustworthy for describing the function of the heart when the body is in horizontal position. The function of the heart is not identical in upright position and this must be kept in mind.

The fact that only two different hearts were modelled makes it impossible to draw any general conclusions concerning the function of the human heart.

7.2.1 Obstacles along the way

The obstacles that we encountered were expected and not severe. The mitral flow measurement of subject A suffered from a slight misplacement of the measurement planes which led to uncertain flows. The mitral flow was excluded from the graphs due to this.

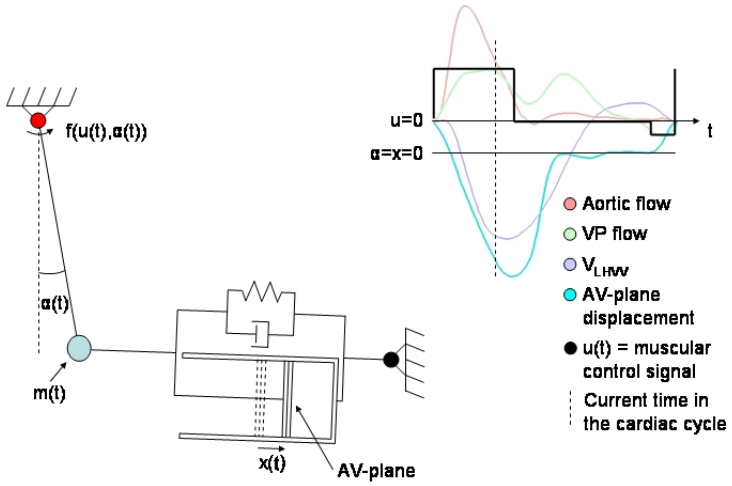

Figure 7.7: A technical model of the pumping mechanics of the heart. The model is built up of a pendulum with variable mass $m(t) = \rho V_{\text{Left Heart}}(t) - \rho V_{\text{Direct Flow}}(t) + C$, where ρ is the density of blood, $V(t)$ is the volume and C is a constant. A spring-damper subsystem that describes the elastic forces, which are related to the passive spring force shown in Figure 4.5a, and viscous friction is placed in parallel with a piston pump. There is an applied torque $f(u(t), \alpha(t))$ that corresponds to atrial contraction if negative and ventricular contraction if positive and $u(t)$ is the muscular control signal. The angular dependence of the torque $f(u(t), \alpha(t))$ is related to the active spring force shown in Figure 4.5b. The angle $\alpha(t)$ is the deviation from the equilibrium position of the pendulum and the equilibrium length of the spring. The equilibrium state of the system corresponds to $\alpha = 0$. The AV-plane position on the axis where the two-chamber, four-chamber and LVOT planes coincide is given by $pos_{\text{AV}}(t) = |x_{\max}(t)| + |x_{\min}(t)| - x(t) + x_{\min}(t)$.

The high cardiac experiment involved the invention of a special harness with rubber bands attached to the feet of subject B in order to reduce motion artifacts during exercise.

The ECG triggering and oximeter triggering caused big problems in the high cardiac experiment. Real time MRI without triggering was the only solution. The lack of triggering made it impossible to fit flows of different vessels in time with necessary accuracy. That is the reason why no V_{LHVV}-plot or pulmonary vein flow plot exist.

There was no possibility of doing a strain analysis in radial coordinates since there was no software supporting it at the time and it would have been too time consuming to implement. If time was not a limitation, this kind of analysis would give answer to the timing of torsion of the left ventricle.

7.2.2 Sources of error

There are several potential sources of error in the 3D-flow analysis. The pathlines were created using a rectangular emitter tool. It would be easier to drop particles that would represent all of the blood particles passing through the plane by using a circular emitter tool. The use of a circular emitter tool is much more time consuming and the positioning of the plane is harder to do. There are visible artifacts due to eddy currents, which have greatest effect in the outer regions of the 3D-volume, see Figure 6.4. The eddy current artifacts explain why the pathlines from the mitral valve are scattered in the regions of the pulmonary veins. Time invariant eddy current compensation was performed during reconstruction of the 3D data sets of subject A. Time variant eddy current compensation was performed during reconstruction of the 3D data sets of subject B. The difference in suppressing artifacts between the two methods seem to be limited. The comparison of the 3D-flows between the two subjects would benefit it the same compensation was performed in both cases. The temporal and spatial resolution limits the accuracy. The consistency of a backward pathline compared to a forward pathline was tested. The presence of noise affected the result, which is shown in Figure 7.8. Respiration may have caused motion artifacts.

One of the sources of error involved in cine MRI could be respiration artifacts even though a breathhold technique was used. The temporal and spatial resolution limit the accuracy. Accurate and consistent positioning of measurement planes is crucial for good results. Respiration artifacts are most likely present in flow MRI. The temporal and spatial resolution limit the accuracy. Accurate and consistent positioning of measurement planes is crucial for good results. The absence of mitral flow in the graphs of subject A is due to bad positioning of measurement planes. Eddy currents can cause artifacts. The choice of velocity encoding is important in order to capture the flow information of interest. The cine and flow MRI data acquisition of the subjects should preferable be done on the same MR-scanner in order to reduce the sources of error that could affect the result of a comparison between the different hearts.

High cardiac output experiment could also have been affected by eddy currents. Motion artifacts caused by inspiration give rise to slight disturbances in flow magnitude. The error will have limited effect since the flow is averaged over 5 cycles at rest and 6 cycles during work. The inspiration causes changes of the volume of the heart. In order to improve the reliability of the result, it would be good if the duration of the acquisition lasted at least one pulmonary cycle. The temporal and spatial resolutions are limitations, but the use of upsampling before spatial averaging improves the signal to noise ratio.

Manual segmentation involves subjective definitions of borders. VPDI and VPDS of subject A was segmented manually twice in order to get a measure of the subjectivity. The difference in accumulated flow during one cardiac cycle was 2.1% for VPDI and 1.0% for VPDS. The velocity encoding makes it possible to get aliasing effects, but most of the artifacts were hopefully removed by the anti-aliasing algorithms used in Segment.

The flow and kinetic energy calculations of the hearts of subject A and subject B involves sources of error. The flow and kinetic energy calculations of subject A was based on flow MRI data that was acquired at an average heart rate of 61 bpm (56 bpm - 63 bpm). The stroke volume differed slightly between inflow and outflow. The stroke volume according to aortic flow measurement was 117.5 ml and 120.7 ml according to pulmonary flow measurements. The difference was 2,7%. The flow and kinetic energy calculations of subject B was based on flow MRI data that was acquired at an average heart rate of 56 bpm (52 bpm - 61 bpm). The heart rates during cine

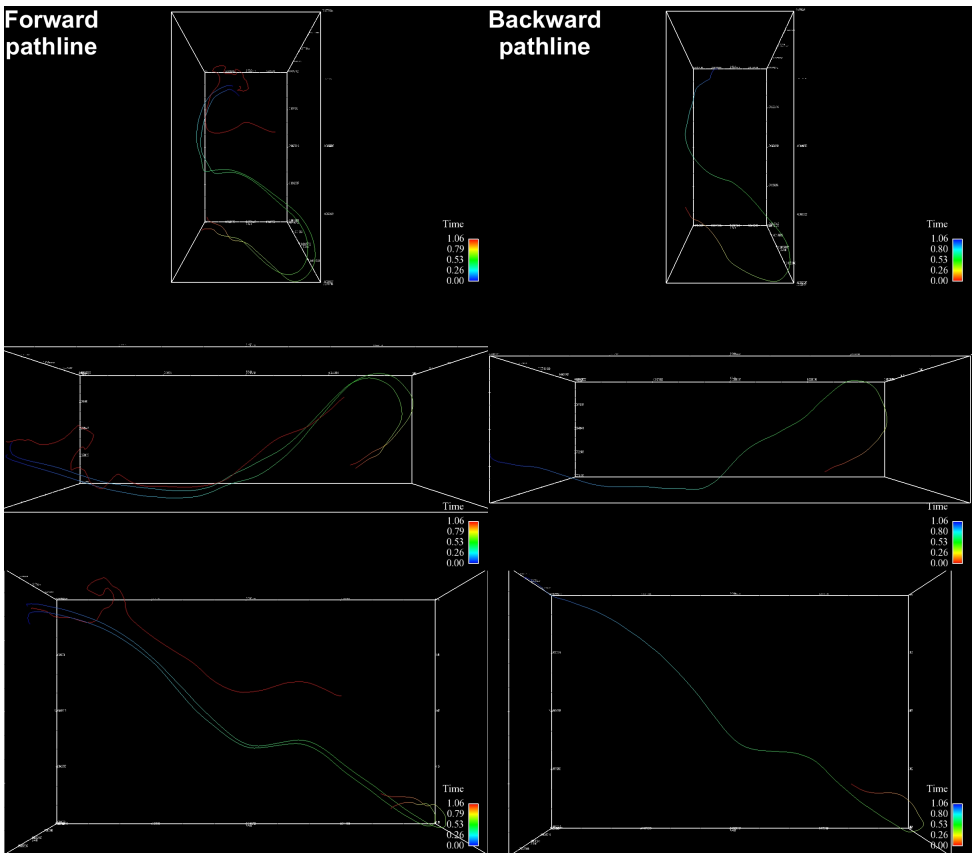

Figure 7.8: This is a comparison of pathlines forward and backward in time using Ensight 8.2. The right hand panels show a backward pathline from x, y and z perspective. The coordinates of the start and the endpoint were noted in order to create a corresponding pathline using forward time. The result is shown in the left panels. When a particle was dropped exactly from the end point of the backward pathline, the result was unsatisfactory due to noise. If particles were dropped just a small distance from the start point of the first try, the pathlines turned out similar to the backward pathline. The unsatisfactory pathline is the one marked with red color. Ensight uses a 2-2 Runge Kutta method [6]. The technique has visible limitations when the spatial and temporal resolutions are low and noise is present. Unrealistic pathlines do occur, but not frequently.

MRI data acquisition were four-chamber: 52 bpm, two-chamber: 52 bpm and LVOT 55 bpm. The stroke volume according to aortic flow measurement was 106.7 ml and 103.5 ml according to pulmonary flow measurements. The difference was 2,8%. The difference in heart rates was compensated for in the initiation of the model, where the time dependent data is scaled to fit the average time increment of all flows. The difference between incoming volume and outgoing volume is removed by scaling the cross section area of the pulmonary veins. That is an approximation that will compress or expand the velocity profile of the pulmonary flow radially. It would be more accurate to rearrange the velocity profile of the flow both in radial direction and in the direction

of the flow, but calculating a proper ratio is not trivial. If the difference in inflow and outflow is only dependent on manual segmentation, the radial shape of the velocity profile should be cropped when the flow is too large and extrapolated when it is too small in order to fit the true cross section area.

The interpolation of the mitral flow could suffer from nonlinearities of the AV-plane movement due to mismatch of heart rates.

The filtering of the flow, kinetic energy and position data could disguise information. The filter used is a non-causal gauss filter which should not give rise to any significant changes in the periodic pattern of the data, only gentle smoothening. The slight aortic backflow in early diastole is disguised by filtering, which is not desired.

7.3 Conclusions

This thesis gives a hint about the importance of involving engineering skills into medicine and vice verse in order to improve the understanding of cardiac physiology and subsequent patient treatment strategies.

The mathematical model developed is based on balance equations that guarantee that the model is valid as long as the underlying assumptions are realistic.

The Matlab/Simulink-model uses accepted methods for flow measurements but assembled in new ways in order calculate concurrent flows, kinetic energy of flows and volume variations.

By using the modelling approach described in this thesis, it should be possible get a good view of the functionality of a heart based on true flows and corresponding kinetic energy of a heart within two hours. The power of the technique will increase as research makes it possible to relate the results to the properties of healthy hearts.

The properties of thorax and the cardiovascular system are involved in the pumping mechanism in ways that make it misleading to explain the heart as an isolated and inflow controlled pump. The contributions from pressures, elastic strain energy and kinetic energy inside and outside of the heart to the pumping mechanism cannot be measured or verified by single measurements, which makes it necessary to do research with several different experiments in parallel in order to box in the most important contributions. Some ideas for future research are presented in section 7.4.

This thesis presents a novel foundation for future modelling of the dynamics of the human heart based on fluid mechanics that is not limited to current theories in cardiovascular physiology.

7.4 Future work

This section presents ideas for future work.

- 3D-flow analysis at high cardiac output
- Total heart volume variation analysis at high cardiac output
- Modelling the valves based on the new theories
- Model the left atrium with the mitral valve open during the whole cardiac cycle with the finite element method in order to estimate the kinetic energy losses due to friction. This makes it possible to estimate the contribution from the atrial vortex to the energy efficiency of the heart.

- Investigate the timing of arterial reflexes at different work loads and the impact of them
- Investigate the AV-plane curve as a property of age due to the change of elastic properties of the large vessels and the heart when aging
- Relate the heart rate dependent switch to sinusoidal AV-plane displacement to the anaerobic threshold.
- Different approaches of cardiac surgery based on the age of the patient due to the changes in elastic properties and thus, stroke length of the AV-plane and timing of reflections of pressure waves in the artery tree
- Develop automated segmentation methods for 3D-flow volumes with automatic visualization of all flows and all important events in time simultaneously. This would make it possible for cardiac surgeons to take part of the flow information available in order to improve custom made high precision surgery
- Investigate how the function of the heart depends on ventricular volume. This should be done by looking at direct/retained flow ratio and AV-plane displacement. Does an oversized ventricle cause lower velocities? Are opposing flows more common when the ventricular contraction passes on a smaller amount of energy per unit blood mass?
- It is not possible to measure the energy that the retained flow contributes to the pumping movement, but it is possible to calculate the mass of the retained flow. The understanding of the pumping mechanics might be improved by comparing the mass of the retained flow at different cardiac output
- Relate AV-plane displacement to the valve function, and thereby retained flow by looking at normal function and the function of hearts with aortic valve insufficience
- Investigate the change of function of the heart as the atrial contraction is temporarily disabled in patients with dilated atrium. What happens to the AV-plane displacement and the kinetic energy of the aortic flow and the pulmonary vein flows? Is there any direct flow?
- Investigate the contribution of left ventricular torsion to the AV-plane displacement of the right heart. Does the rotation change the lever of the muscles in the right ventricle, which could contribute to the larger displacement on the right side than the left side?

Chapter 8

Notations

$\hat{\mathbf{n}}$ is the unit surface normal pointing outwards of the volume.
$\mathbf{x} = \mathbf{x}(\mathrm{x}, \mathrm{y}, \mathrm{z})$ is the position
$\mathbf{r} = \mathbf{x} - \mathbf{x_P}$ is the distance between an arbitrary position and the point $\mathbf{P}$
$\mathbf{v} = \mathbf{v}(\mathrm{x}, \mathrm{y}, \mathrm{z}, \mathrm{t})$ is the absolute velocity
$\mathbf{a} = \mathbf{a}(\mathrm{x}, \mathrm{y}, \mathrm{z}, \mathrm{t})$ is the absolute acceleration
$\mathbf{v}_\mathrm{r} = \mathbf{v}_\mathrm{r}(\mathrm{x}, \mathrm{y}, \mathrm{z}, \mathrm{t})$ is the relative velocity
$\mathbf{v_s} = \mathbf{v_s}(\mathrm{x}, \mathrm{y}, \mathrm{z}, \mathrm{t})$ is the velocity of a surface
$\mathbf{a} = \mathbf{a}(\mathrm{x}, \mathrm{y}, \mathrm{z}, \mathrm{t})$ is the absolute acceleration
$\mathbf{a}_\mathrm{r} = \mathbf{a}_\mathrm{r}(\mathrm{x}, \mathrm{y}, \mathrm{z}, \mathrm{t})$ is the relative acceleration
$\mathbf{R}$ is the origin of a moving coordinate system
$\mathbf{\Omega}$ is absolute angular velocity
S is the entropy
V is the volume
V_{THVV} is the total heart volume variation
V_{LHVV} is the left heart volume variation
V_{RHVV} is the right heart volume variation
V_{SCSVV} is the systemic circulatory system volume variation
V_{PCSVV} is the pulmonary circulatory system volume variation
T is the torsion
τ is the shear stress
θ is the angle that apex rotates relative the rather fixed basal part of the left ventricle in a cylindrical coordinate system. G is the shear modulus
L is the length

$\varphi_{\text{mitral}}(t)$ is the mitral valve function
$W(t)_{\text{VC}}$ is the work done by ventricular contraction
$W(t)_{\text{ESE}}$ is the work done by elastic strain energy
$W(t)_{\text{AC}}$ is the work done by atrial contraction
m is the mass
ρ is the density
q is the flow
A is the area
H is the angular moment
E is energy
e is the system energy per unit mass
pos_{AV} is the spatially averaged position of the AV-plane on the axis where the two chamber, four chamber and LVOT plane coincide.

Chapter 9

Glossary

anterior	in front
apex	the tip of the heart
apical	towards apex
atrio-ventricular plane (AV-plane)	the plane that divides the heart in atria and ventricles
basal	towards the base, the opposite to apical
direct flow	the flow that enters and leaves the ventricle within one cardiac cycle
endocardium	the thin serous membrane that lines the interior of the heart
epicardium	the inner layer of the pericardium which is in contact with the heart
lateral	on the side
myocardium	the muscular tissue of the heart
myocyte	a muscle cell
pericardium	the membranous sac filled with serous fluid that encloses the heart
posterior	to the rear
retained ejection flow	the portion of blood inside of the ventricle that is accelerated by the ventricular contraction but does not pass through the aortic valve
retained flow	the flow that does not enter and leave the ventricle within one cardiac cycle

sagittal plane	divides the body in symmetric left and right halves
septal	related to septum
septum	a membrane that divides two cavities
thorax	the chest
vasoconstriction	the constriction of a blood vessel, stimulated by nerve signals or hormones
vasodilation	the dilation of a blood vessel, stimulated by nerve signals or hormones
VPSS	the upper left pulmonary vein
VPSI	the lower left pulmonary vein
VPDS	the upper right pulmonary vein
VPDI	the lower right pulmonary vein

References

[1] P. Benham, R. Crawford, and C. Armstrong. *Mechanics of engineering materials*. Pearson Education Limited, Harlow, Second edition, 1996.

[2] A. F. Bolger, E. Heiberg, A. Sigfridsson, J. Kvitting, M. Karlsson, and L. Wigstrom. Subset analysis of global left ventricular blood flow. In *SCMR*, San Francisco, 2005.

[3] C. Carlhall, L. Wigstrom, E. Heiberg, M. Karlsson, A. F. Bolger, and E. Nylander. Contribution of mitral annular excursion and shape dynamics to total left ventricular volume change. *Am J Physiol*, 287:1836–1841, 2004.

[4] M. Carlsson, P. Cain, C. Holmqvist, F. Stahlberg, S. Lundback, and H. Arheden. Total heart volume variation throughout the cardiac cycle in humans. *Am J Physiol*, March 2004.

[5] M. Carlsson, M. Ugander, H. Mosén, T. Buhre, and H. Arheden. Longitudinal antrioventricular plane displacement is the major contribution to left ventricular pumping in healthy adults, athletes and patients with dilated cardiomyopathy. *Am J Physiol*, 287:243–250, November 2006.

[6] D. L. Darmofal and R. Haimes. An analysis of 3d particle path integration algorithms. *Journal of Computational Physics*, 123:182–195, 1996.

[7] N. Fukuda and H. L. Granzier. Titin/connectin-based modulation of the frank-starling mechanism of the heart. *Heart and Vessels*, 26:319–323, 2005.

[8] A. Fyrenius, L. Wigstrom, T. Ebbers, M. Karlsson, J. Engvall, and A. F. Bolger. Three dimensional flow in the human left atrium. *Heart*, 86:448–455, 2001.

[9] H. L. Granzier and S. L. and. The giant protein titin: A major player in myocardial mechanics, signaling and disease. *Circ. Res.*, 94:284–295, 2004.

[10] R. Hainsworth and M. Drinkhill. Counterpoint: Active venoconstriction is not important in maintaining or raising end diastolic volume and stroke volume during exercise and orthostasis. *J Appl Physiol*, 101:1264–1265, 2006.

[11] E. Heiberg, T. Ebbers, L. Wigstrom, and M. Karlsson. Three-dimensional flow characterization using vector pattern matching. *IEEE transactions on visualization and computer graphics*, 9:313–319, 2003.

[12] E. Heiberg, K. Markenroth, and H. Arheden. Validation of free software for automated vessel delineation and mri flow analysis. In *SCMR*, Rome Italy, 2007.

[13] N. B. Ingels. Myocardial fiber architecture and left ventricular function. *Technology and Health Care (IOS Press)*, 5:45–52, 1997.

[14] B. Jonson and P. Wollmer. *Klinisk fysiologi med nuklearmedicin och klinisk neurofysiologi*, pages 137–144. Liber AB, Stockholm, Second edition, 2005.

[15] P. J. Kilner, M. Y. Henein, and D. G. Gibson. Our tortuous heart in dynamic mode - an echocardiographic study of mitral flow and movement in exercising subjects. *Heart and Vessels*, 12:103–110, 1997.

[16] P. J. Kilner, G.-Z. Yang, and D. N. Firmin. Morphodynamics of flow through sinous curvatures of the heart. *Biorheology*, 39:409–417, 2002.

[17] P. J. Kilner, G.-Z. Yang, A. J. Wilkes, R. H. Mohladdin, D. N. Firmin, and M. H. Yacoub. Asymmetric redirection of flow through the heart. *Nature*, 404:759–761, 2000.

[18] M. M. LeWinter, Y. Wu, S. Labeit, and H. L. Granzier. Cardiac titin: Structure, functions and role in disease. *Clinica Chimica Acta*, 375:1–9, 2007.

[19] M. Lichtwarck-Aschoff, B. Suki, A. Hedlund, U. H. Sjostrand, A. Markstrom, R. Kwatai, G. Hedenstierna, and J. Guttmann. Decreasing size of cardiogenic oscillations reflects decreasing compliance of the respitory system during long-term ventilation. *J Appl Physiol*, 96:879–884, 2004.

[20] S. Lundback. Cardiac pumping and the function of ventricular septum. *Acta Physiol Scand*, 127:8–101, 1986.

[21] M. Malik and A. J. Camm. *Dynamic electrocardiography*, pages 203–206. Futura Blackwell Publishing, Elmsford, N.Y., First edition, 2004.

[22] P. Moran. A flow velocity zeugmatographic interlace for nmr imaging in humans. *Magnetic Resonance Imaging*, 1(4):197–203, 1982.

[23] J. Murray and J. Kennedy. Quantitative angiography. ii. the normal left atrial volume in man. *Circulation*, 37:800–804, 1967.

[24] A. Persson and L.-C. Boiers. *Analys i flera variabler*, pages 334–343. Studentlitteratur, Lund, Second edition, 1996.

[25] R. F. Rushmer. *Cardiovascular dynamics*, pages 63–69. W.B. Saunders Company, Philadelphia and London, Second edition, 1961.

[26] D. V. Schroeder. *An introduction to thermal physics*, pages 108–113. Addison Wesley Longman, San Francisco, First edition, 2000.

[27] N. Stergiopulos, B. E. Westerhof, and N. Westerhof. Total arterial inertance as the fourth element of the windkessel model. *Am J Physiol*, 276:81–88, 1999.

[28] A. Vander, J. Sherman, and D. Luciano. *Human physiology: the mechanisms of body function*, pages 407–452. McGraw Hill, Boston, Eighth edition, 2001.

[29] A. Weyman. *Principles and practice in echocardiography*, pages 471–491. Lea and Febiger, Philadelphia, Second edition, 1994.

[30] F. M. White. *Fluid mechanics*. McGraw-Hill, New York, Fifth edition, 2005.

[31] L. Wigstrom, T. Ebbers, A. Fyrenius, M. Karlsson, J. Engvall, B. Wranne, and A. F. Bolger. Particle trace visualization of intracardiac flow using time-resolved 3d phase contrast mri. *Magnetic Resonance in Medicine*, 41:793–799, 1999.

[32] L. Wigstrom, L. Sjoqvist, and B. Wranne. Temporally resolved 3d phase-contrast imaging. *Magnetic Resonance in Medicine*, 36:800–803, 1996.

Appendix A

Simulink model

A.1 Initiation

In order to make the Simulink-model relatively user friendly, two linked initiation files are used. Pulmonary vein flow data, mitral flow data and aortic flow data should be pasted into the first initiation file. If the user puts the AV-plane segmentation files in the same folder as the model, the AV-plane position data will be extracted automatically. The second initiation file makes the data to fit the model interface. All flow based data is scaled with the fraction between its original sample time and the average sample time of all flows. The data is then upsampled, which is especially important for the calculation of mitral flow. The AV-plane position measured in LVOT, two chamber and four chamber is spatially averaged. All input data is expanded to three periods and then filtered by using the following Gaussian

$$f(i) = \frac{1}{\sum_{j=1}^{7} a(j)} e^{-\frac{(a(i))^2}{2}} \tag{A.1}$$

where $a = [-3 \dots 3]$. The mid period is extracted in order to get continuous filtered periodic data.

A.2 Model

The model consists of several subsystems, the time generator, the AV-position subsystem, the flow data subsystem, the energy subsystem and volume subsystem, see Figure A.1.

A.2.1 Time generator

All of the time dependent data that is used in the model is accessed from lookup tables. In order to make the lookup tables compatible as sources in periodic sequences, a time generator that creates a sawtooth wave with the an amplitude corresponding to the length of the data vectors is used. It allows an arbitrary running time.

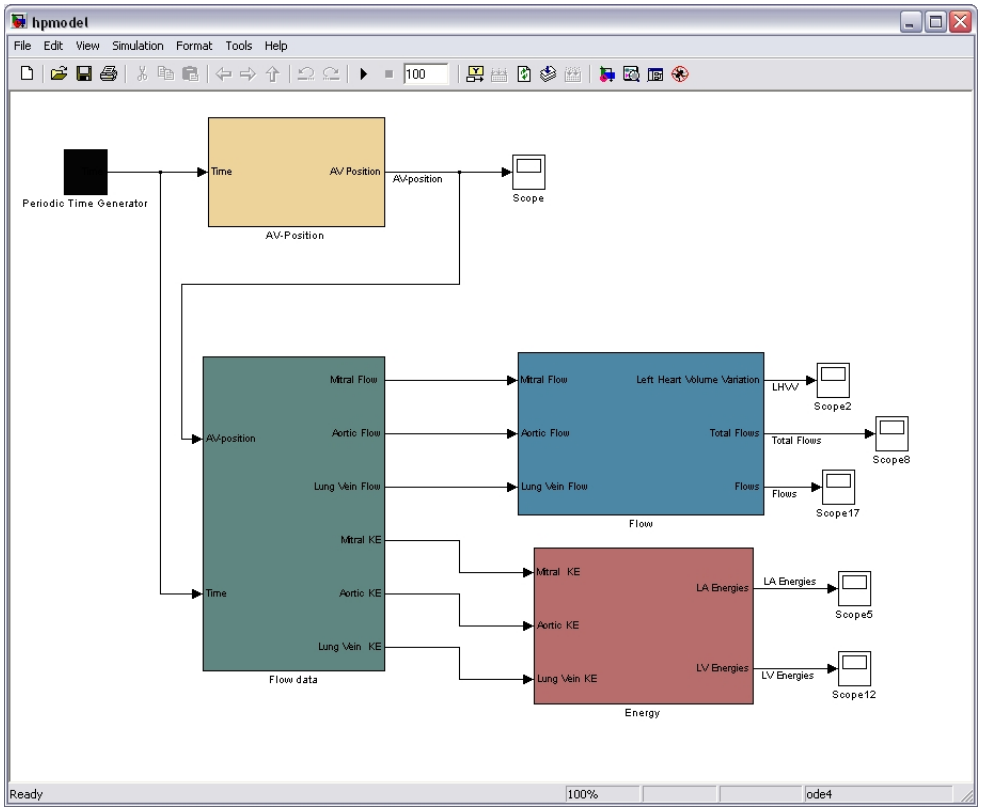

Figure A.1: The model consists of several subsystems, the time generator, the AV-position subsystem, the flow data subsystem, the energy subsystem and volume subsystem.

A.2.2 AV-position subsystem

The subsystem contains a AV-plane position lookup table. The outputs are the AV-plane position and the time derivative of the position, the velocity of the AV-plane.

A.2.3 Flow data subsystem

The aortic flow block contains two lookup tables, one for flow and one for energy of the flow. The flow data subsystems contains three subsystems, the pulmonary vein block, the aortic block and the mitral block. The pulmonary vein subsystem contains one flow lookup table and one energy lookup table for each pulmonary vein. The pulmonary flow will be balanced in every second run in order to get the same accumulated flow as the more accurate aortic flow. The mitral subsystem contains one flow lookup table, one energy lookup table and one cross section area lookup table for each of the two mitral flow measurements. The two mitral flows are used to get an interpolated mitral flow based on AV-plane position. (Figure A.2) The weights are adjusted depending on the AV-plane position. The basal mitral flow measurement will be the only contribution taken into account when the AV-plane is in its most basal position. Correspondingly, the apical measurement will be the only contribution when the AV-plane is in its most

apical position. For all positions in between, the flows are linearly interpolated. The energies and cross section areas are interpolated with the same weights. For the mitral flow, the following approximation is used

$$\int (\mathbf{v} \cdot \hat{\mathbf{n}})\, dA \approx \frac{pos_{\mathrm{AV}}}{pos_{\mathrm{AV\,max}}}\, q_{\mathrm{mitral\,1}} + (1 - \frac{pos_{\mathrm{AV}}}{pos_{\mathrm{AV\,max}}})\, q_{\mathrm{mitral\,2}}, \qquad 0 < pos_{\mathrm{AV}} < pos_{\mathrm{AV\,max}} \tag{A.2}$$

where $q_{\mathrm{mitral\,1}}$ is the absolute flow through the basal mitral measurement plane, $q_{\mathrm{mitral\,2}}$ is the absolute flow through the apical mitral measurement plane and pos_{AV} is the position of the AV-plane. The mitral valve block inside of the mitral flow block is the part that simulates the behaviour of the valve. The mitral valve is not open during systole. The start of diastole is defined in the model as the timeframe of the AV-plane position minimum. The interpolated flow corresponds to a moving measurement point that measures absolute flow. The absolute flow is used in order to calculate the energy of the blood that flows through the mitral valve. The movement of the mitral valve will make a volume of blood, that previously belonged to the left atrium, to belong to the left ventricle.

$$\int (\mathbf{v}_{\mathrm{r}} \cdot \hat{\mathbf{n}})\, dA = \int ((\mathbf{v} - \mathbf{v}_{\mathrm{mitral\,valve}}) \cdot \hat{\mathbf{n}})\, dA \tag{A.3}$$

where $\mathbf{v}_{\mathrm{r}}$ is the relative velocity, $\mathbf{v}$ the absolute velocity and $\mathbf{v}_{\mathrm{mitral\,valve}}$ is the velocity of the mitral valve which is approximated to

$$\mathbf{v}_{\mathrm{mitral\,valve}} \approx \frac{dpos_{\mathrm{AV}}}{dt} \tag{A.4}$$

where pos_{AV} is the position of the AV-plane. It should be kept in mind that $\mathbf{v}_{\mathrm{mitral\,valve}}$ and $\mathbf{v}$ have opposite signs. The contribution from $\mathbf{v}_{\mathrm{mitral\,valve}}$ to the change of volume should not be used in energy calculations since its is only a question of changing borders, not absolute flow.

A.2.4 Flow subsystem

The flow subsystem combines the flows of the left atrium and the left ventricle so that they can be plotted in one scope respectively. In order to get accumulated flows, the flows are scaled and integrated over time. The scaling is done so that the output will be in SI units, even though the integer step of the running time is not in seconds. The left heart volume variation is obtained by subtracting the aortic accumulated flow from the accumulated pulmonary vein flow.

A.2.5 Energy subsystem

The energy subsystem integrates the kinetic energy of the flows over time in order to visualize the incoming energy and outgoing energy of the left atrium and the left ventricle. The minimum work that is needed to balance the incoming kinetic energy and outgoing kinetic energy over a cardiac cycle is calculated by subtracting the outgoing accumulated energy from the incoming accumulated energy of the left atrium and left ventricle respectively.

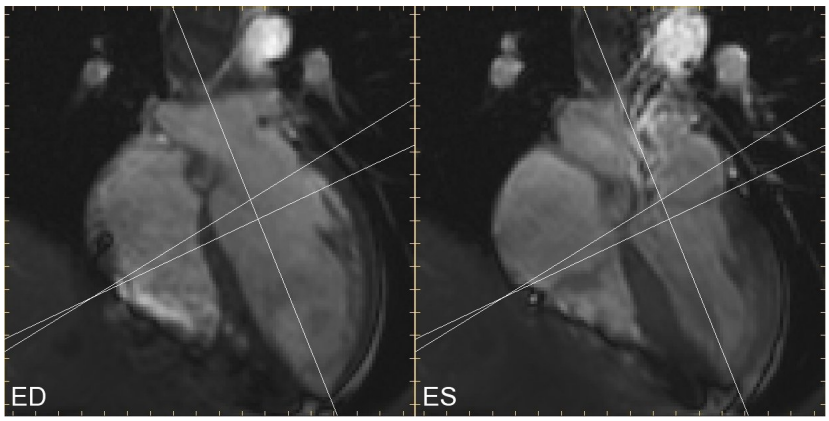

Figure A.2: Four-chamber image in end diastole to the left and the corresponing image in end systole to the right. The horizontal lines are the two mitral planes and the vertical shows the orientation of the two-chamber image.